Polymer-Based Optical Guided-Wave Biomedical Sensing: From Principles to Applications

photonics

MDPI

Review

Polymer-Based Optical Guided-Wave Biomedical Sensing: From Principles to Applications

Malhar A. Nagar and Davide Janner *

Dipartimento di Scienza Applicata e Tecnologia (DISAT), Politecnico di Torino, C.so Duca degli Abruzzi 24, 10129 Turin, Italy; malhar.nagar@polito.it

* Correspondence: davide.janner@polito.it

Abstract: Polymer-based optical sensors represent a transformative advancement in biomedical diagnostics and monitoring due to their unique properties of flexibility, biocompatibility, and selective responsiveness. This review provides a comprehensive overview of polymer-based optical sensors, covering the fundamental operational principles, key insights of various polymer-based optical sensors, and the considerable impact of polymer integration on their functional capabilities. Primary attention is given to all-polymer optical fibers and polymer-coated optical fibers, emphasizing their significant role in "enabling" biomedical sensing applications. Unlike existing reviews focused on specific polymer types and optical sensor methods for biomedical use, this review highlights the substantial impact of polymers as functional materials and transducers in enhancing the performance and applicability of various biomedical optical sensing technologies. Various sensor configurations based on waveguides, luminescence, surface plasmon resonance, and diverse types of polymer optical fibers have been discussed, along with pertinent examples, in biomedical applications. This review highlights the use of biocompatible, hydrophilic, stimuli-responsive polymers and other such functional polymers that impart selectivity, sensitivity, and stability, improving interactions with biological parameters. Various fabrication techniques for polymer coatings are also explored, highlighting their advantages and disadvantages. Special emphasis is given to polymer-coated optical fiber sensors for biomedical catheters and guidewires. By synthesizing the latest research, this review aims to provide insights into polymer-based optical sensors' current capabilities and future potential in improving diagnostic and therapeutic outcomes in the biomedical field.

Keywords: biomedical sensing; luminescence sensors; polymer-based fiber Bragg gratings (PFBGs); polymer-based optical fiber sensors (POFs); surface plasmon resonance (SPR) sensors; waveguide sensors

Citation: Nagar, M.A.; Janner, D. Polymer-Based Optical Guided-Wave Biomedical Sensing: From Principles to Applications. *Photonics* **2024**, *11*, 972. https://doi.org/10.3390/photonics11100972

Received: 7 September 2024
Revised: 11 October 2024
Accepted: 15 October 2024
Published: 17 October 2024

1. Introduction

Polymer-based optical sensors (POS) have become increasingly important in biomedical diagnostics, monitoring, and therapy due to their exceptional properties, such as flexibility, biocompatibility, and selective responsiveness [1–3]. These materials enable the development of sophisticated sensors that meet the rigorous demands of biomedical applications, including real-time health monitoring and clinical diagnostics. The global market for biomedical sensors was estimated to be USD 10.79 billion in 2023 and is projected to reach USD 20.95 billion by 2030, growing at a compound annual growth rate (CAGR) of 15.87% from 2024 to 2030 [4]. Within this sector, global medical fiber optics was valued at USD 4.85 billion in 2023 and is expected to grow to USD 7.32 billion in 2030, with a CAGR of 6.1% [5]. This expected growth of fiber optics in the biomedical sector highlights the critical role these sensors play in improving healthcare outcomes.

The historical development of polymer-based optical sensors can be traced back to advances in optical sensor technology and polymer chemistry in the late 20th century. Polymer optical fibers (POFs) have been an active area of research and development since DuPont first developed them in the 1960s. Researchers began exploring their use for

sensing applications in the 1970s and 1980s due to advancements in polymer chemistry and fiber fabrication techniques, leading to enhanced mechanical and optical properties. In the 1990s and 2000s, there was a surge in research and development leveraging on the advantages of polymers, leading to the use of molecularly imprinted polymers (MIPs) and polymer coatings for various applications. Recent advancements include the use of 3D printed techniques for the fabrication and integration of POS with other technologies, novel materials to enhance POS response to external stimuli, and innovations in distributed sensing [6–10].

In the context of these technological advancements, biomedical sensing has emerged as a critical application area for polymer-based optical sensors. Biomedical sensing refers to the detection and monitoring of biological or physiological parameters using various sensor technologies, often designed to be minimally invasive or non-invasive. These sensors can detect a wide range of biological analytes, such as proteins, DNA, glucose, and various ions, as well as physiological parameters like temperature, pH, and pressure. Biomedical sensors are crucial in applications across healthcare and medicine, including diagnostics, patient monitoring, and personalized medicine. These sensors are employed in a wide range of applications, such as physiological monitoring, health diagnostics, biomechanics, wearable devices, and robotics [1,11–13]. Advances in polymer-based optical sensors have expanded the scope of biomedical sensing, providing new ways to detect and monitor health conditions with high sensitivity and specificity, particularly in the early diagnosis of diseases and in settings requiring portable and cost-effective solutions. In the vast field of polymer-based optical sensing techniques, we have chosen to focus on luminescent sensors, surface plasmon resonance (SPR) sensors, waveguide sensors, POF (all-polymer fibers—the fiber itself is composed entirely of polymer materials), and polymer-coated optical fibers (where the fiber is typically made of glass or silica and is coated with a polymer layer(s)). The combination of these techniques represents the majority of optical techniques that are commonly integrated with polymers to enhance sensor functionalities. They were selected based on their widespread use, significant advancements, and substantial potential for innovation in the biomedical sensing field. These POFs can be optically differentiated based on their ability to measure various characteristics of light, such as intensity, wavelength, and phase. Although state-of-the-art technologies often rely on traditional electrical and electromechanical sensors due to their faster response times, longer lifespan, high repeatability, and reliability, these sensors face significant drawbacks, such as susceptibility to electromagnetic interference (EMI), risks of electrical shocks/sparks, and noise interference. Additionally, they frequently require bulky instrumentation for data acquisition [1]. Consequently, there is a technological shift towards optical-based sensors since they are immune to EMI, have smaller dimensions, and are lightweight, making them easily integrated into catheters, endoscopes, and other medical devices. Their inertness, biocompatibility, and enhanced sensitivity for various measurements ensure long-term stability and remote sensing applications that involve compatibility with telemetry in the healthcare sector [14–16].

Moreover, polymers offer tailored optical properties, including adjustable refractive indices (due to mechanical modifiability, crosslinking, and polymerization techniques), high transparency at operating wavelengths, and mechanical properties, such as lower Young's modulus, lower yield strength, and higher yield strain and strain limits compared to standard silica-based optical fibers. The mechanical and optical properties of certain polymer materials used for optical biomedical sensing are described in Table 1 and Table 2, respectively. These characteristics are essential for effective light propagation, precision sensing, implantability, and integration into medical devices [1,13,17]. The mechanical flexibility of polymers allows sensors to adapt to dynamic biological environments, while some of them ensure biocompatibility, and their chemical structure allows for the functionalization of their surfaces to target specific biological molecules [18–21]. These polymers' characteristics significantly enhance optical sensors' functionality in biomedical sensing applications. Material selection is crucial for optimizing sensor performance. Various polymers, including

biocompatible, hydrophilic, and stimuli-responsive types, impart selectivity, sensitivity, and stability to the sensors. Fabrication techniques, on the other hand, are vital for sensor development. These techniques enhance the interaction between the sensor surface and biological analytes, thereby further improving sensor performance [13,19,22].

Table 1. Mechanical properties of SMF-28 fiber and some polymers commonly used for fabricating or coating optical fibers.

Material	Young's Modulus (GPa)	Poisson's Ratio	Yield Strength (MPa)	Density (g/cm^3)	Thermal Expansion Coefficient ($10^{-6}/°C$)	Elongation at Break (%)
Silica (SMF-28)	72.0–79.1	0.16–0.17	110–200	2.2	0.55	2–5
PDMS	0.00036–0.0026	0.45–0.5	0.7–2.5	0.965–0.982	300–900	100–200
CYTOP	0.68–3	0.3–0.34	35–45	2.03	70–75	-
PMMA	3–3.7	0.35–0.40	60–70	1.17–1.20	70–85	2–10
PS	3.0–3.5	0.33–0.35	35–60	1.04–1.06	60–80	2–4
Polyimide	2.5–4	0.34–0.42	80–120	1.31–1.43	20–30	10–90
PLA	3.7–4.1	0.34–0.40	25–60	1.21–1.29	60–70	4–6

Table 2. Optical properties of SMF-28 fiber and some polymers commonly used for fabricating or coating optical fibers.

Material	Wavelength Range of Operation (nm)	Transmission Loss (dB/cm)	Thermo-Optic Coefficient ($10^{-5}/°C$)	Refractive Index
Silica (SMF-28)	1300–1600	3.5×10^{-6}–2.0×10^{-6} at 1310 nm and 1550 nm	0.72–0.86	1.465–1.468
PDMS	400–1600	1.8–0.027 at 532 nm and 850 nm	−46.6	1.41
CYTOP	850–1550	0.02–0.15 at 1300 nm and 1500 nm	−5	1.34
PMMA	400–700	2.5–0.02 at 633 nm and 650 nm	−12 to −19	1.486–1.49
PS	450–800	0.03 at 670 nm	−10 to −12	1.587
Polyimide (as coating)	1310–1550	-	−12 to −17	1.60–1.68
PLA	600–850	0.02–0.26 dB/cm from 405–520 nm	-	1.35–1.45

This review aims to provide an overview of various polymer-based optical sensing technologies, offering key insights into their potential use in the biomedical discipline. Building on existing reviews, which provide a comprehensive understanding and usage of polymeric materials for specific optical sensors for biomedical applications, this review classifies POS based on various optical sensing methodologies and highlights the significant impact of polymers in their role and functionality. Polymers, in conjunction with optical waveguides and fibers, enable various biomedical sensing applications by enhancing their performance and applicability. Figure 1 illustrates a comprehensive classification of polymer-based sensors. We start with a comprehensive overview of the fundamental principles behind various polymer-based optical sensor (POS) configurations, covering multiple sensor types, including those based on waveguides, luminescence, SPR, and optical fibers (OFs) designed for both single-point and multi-point sensing applications. Special attention is given to the optical configurations utilized in polymer optical fiber sensors, particularly polymer fiber Bragg gratings (PFBGs) and polymer-coated FBGs, to illustrate their sensing mechanisms and applications in biomedical contexts. The discussion then explores how polymers, when coated onto optical fibers, enhance biomedical sensing capabilities through different optical configurations. This section covers a range of polymeric materials—such as biodegradable, biocompatible, hydrophilic, stimuli-responsive, conductive, and molecularly imprinted polymers—and highlights their functional roles in various biomedical applications. The discussion extends to fabrication techniques for POFs, including thermal drawing, extrusion, laser writing, microfabrication, and advanced coating processes, analyzing their advantages and disadvantages. Key case studies are also highlighted to showcase the effectiveness of polymer-coated optical fiber sensors for

biomedical catheters and guidewires, which can potentially be used in minimally invasive physiological monitoring.

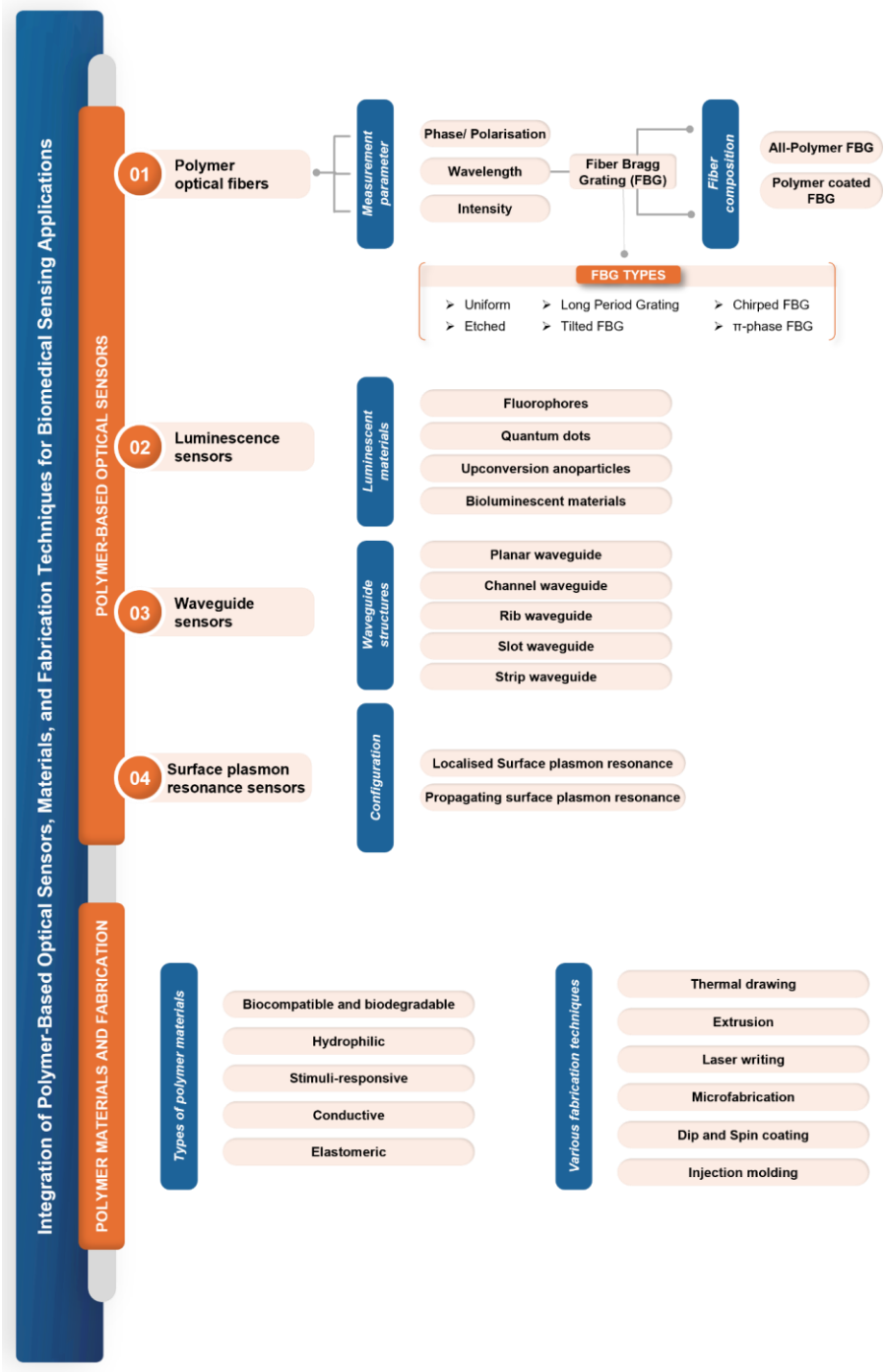

Figure 1. Different classes of polymer-based optical fiber sensors.

2. Polymer-Based Optical Sensors: Concepts and Practices

2.1. Basic Characteristics of Polymer-Based Optical Sensors

Polymers such as poly(methyl methacrylate) (PMMA), polycarbonate (PC), polystyrene (PS), polyimide, amorphous fluorinated polymer (CYTOP), and others possess a diverse set of characteristics that make them ideal for a wide array of biomedical applications. These sensors are incredibly flexible, with Young's modulus ranging from a few MPa to a few GPa. They have high resistance to permanent deformation (yield strain 1–6%) and are lightweight, allowing for seamless integration into wearable and portable de-

vices [3,21,23,24]. Polymers also feature customizable optical properties, such as refractive index and transparency, enabling efficient light propagation and adequate signal loss (0.2–2 dB/cm in specific regions of near-infrared (NIR) and visible wavelengths, mentioned in Table 2) for sensing applications. Figure 2 depicts the characteristic attenuation spectra of POFs based on different materials. The spectra are presented over the wavelength range of 400–1600 nm, encompassing both visible and NIR regions (650 nm–1550 nm) of biological tissue optical window where light penetration is maximized due to reduced scattering and absorption. High attenuation in certain POFs, such as PMMA, at wavelengths beyond 600 nm is due to intrinsic absorption peaks from the fundamental and higher harmonic vibrational modes of molecular bonds within the polymeric material, such as C-H (carbon–hydrogen) and O-H (oxygen–hydrogen). Notably, fluorinated polymers exhibit lower optical losses since hydrogen atoms are replaced with fluorine atoms, reducing vibrational overtones associated with C-H bonds and thereby enhancing transparency in the visible and NIR regions [25]. Moreover, they are known for their chemical and physical stability, making them resistant to various chemicals and thermally stable over a wide range of temperatures [11,19]. Additionally, their ease of fabrication through techniques like molding, hot embossing, and 3D printing allows for customized designs, while surface functionalization facilitates selective detection of specific analytes [26–30]. With the added benefits of cost-effectiveness, environmentally friendly fabrication techniques, and scalability in manufacturing, POS is an appealing choice for mass production [19]. Biocompatible polymers such as polydimethylsiloxane (PDMS), polylactic acid (PLA), polyglycolic acid (PGA), and cellulose, amongst others, are particularly valuable for biomedical and biosensing applications, including implantable and wearable health monitors [2,31]. Furthermore, sensors based on these polymers can be seamlessly integrated with flexible semiconductor electronics and combined with other sensing technologies to create multifunctional platforms [19,32,33]. These combined characteristics make polymer-based optical sensors highly versatile and widely applicable.

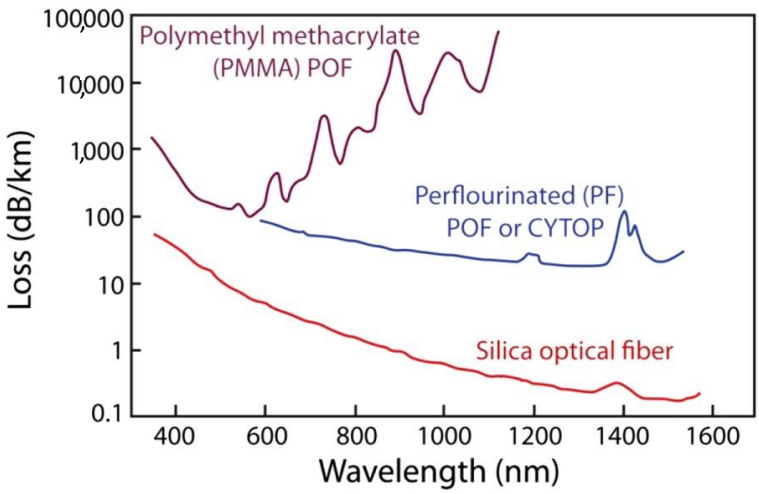

Figure 2. Attenuation characteristics of polymer optical fibers made from different materials: PMMA (polymethyl methacrylate), perfluorinated polymer fiber, and standard silica optical fibers. Reprinted with permission from [34].

2.2. Overview of Types of POS

2.2.1. Waveguide-Based Sensors

Polymer-based optical waveguides (POW) are dielectric structures that operate on the principle of total internal reflection, where light is confined within a high refractive index core surrounded by a lower refractive index cladding. The core-cladding structure guides light with minimal loss while the waveguide is fabricated on a substrate that provides mechanical support. POWs can operate either in single-mode (core diameter: 2–5 μm) or multimode (core diameter: 30–500 μm). These waveguides can withstand bending

and twisting and are extremely flexible compared to traditional waveguides made from inorganic materials, making them apt for portable and biocompatible devices [19,35]. POWs also provide a feasible platform for optical connectivity since they are easily adaptable to on-board and on-chip integration with relatively low propagation loss of <1 dB/cm in the visible and near-infrared regions [36–39].

Planar waveguides, consisting of thin polymer layers on substrates, are extensively used in biosensors and lab-on-a-chip devices for monitoring biological interactions [40]. Channel waveguides, formed by etching or patterning polymers, and rib waveguides, which feature raised ridges for enhanced light confinement, are used in precise light control diagnostic tools [41]. Strip waveguides, having a central polymer strip with a higher refractive index exposed polymer, facilitate surface-based biosensing of refractive index for detection of biomolecules by confining light in both lateral and vertical directions in a broad high refractive index region. Graded-index waveguides, including virtual optical waveguides, with a gradient refractive index change minimize dispersion and enhance light confinement for targeted therapeutic light delivery and label-free biosensing [42,43], as shown in Figure 3a–e. Slot waveguides, characterized by a narrow gap within the polymer core, instead confine light in narrower low refractive index regions, offering high sensitivity for detecting low concentrations of biomolecules. This geometry enhances the overlap between the optical mode and analyte filling the slot, whereas polymer core materials like benzocyclobutene (BCB) and (SU-8) with PMMA as cladding amplify this effect by providing favorable optical properties such as high refractive index contrast and low optical loss. This synergetic enhancement enables sensitivity of 19,280 nm/RIU and 16,500 nm/RIU for BCB and SU-8 core, respectively [44], as depicted in Figure 3f. Flexible and stretchable waveguides, made from hydrogels, elastomers (e.g., PDMS), and biodegradable polymers (agarose, cellulose, PLA, PGA, etc.), are essential for wearable and implantable devices, maintaining sensing performance under large deformations and dynamic conditions [11]. Photonic crystal waveguides utilize periodic structures to control light propagation, enabling advanced sensing with high specificity [45]. These diverse waveguide types meet the specific needs of biomedical applications, enhancing detection, monitoring, and treatment capabilities in healthcare.

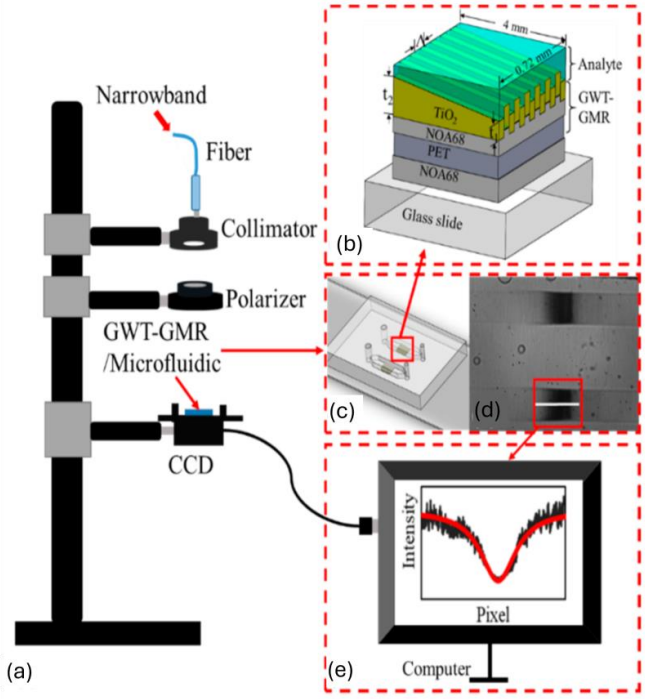

Figure 3. *Cont.*

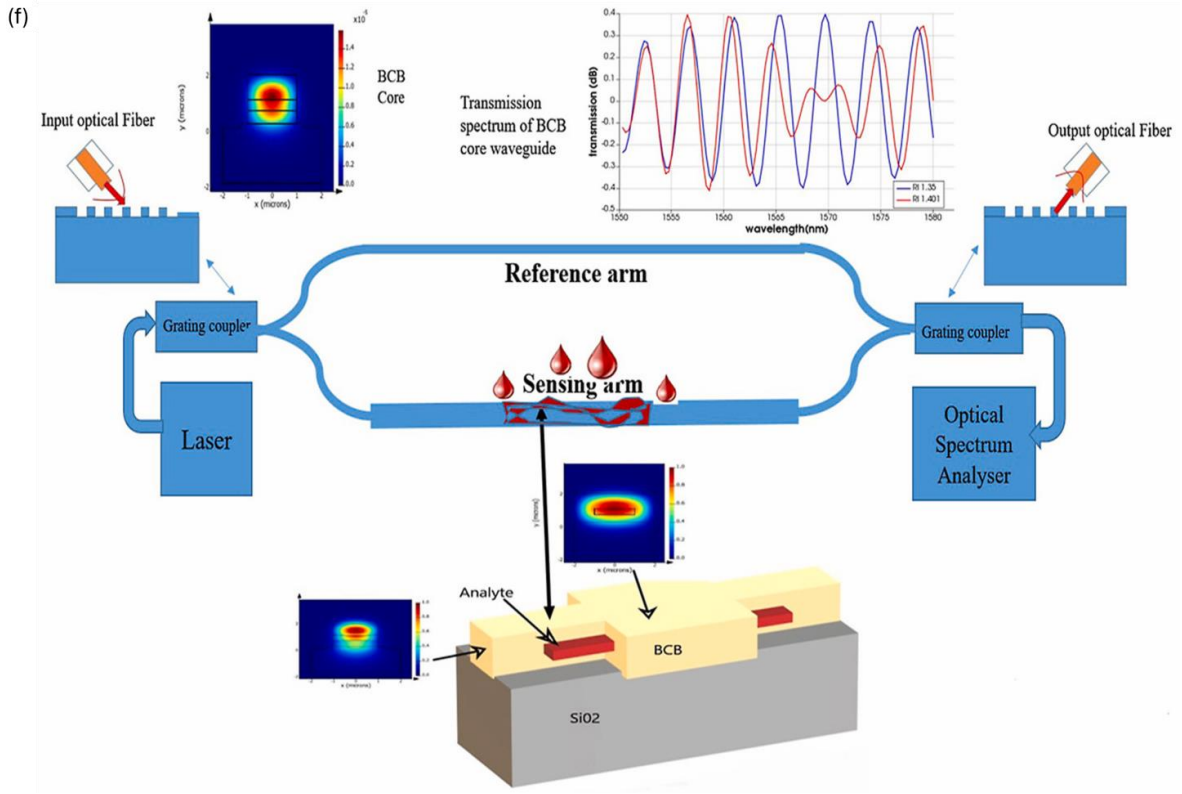

Figure 3. (**a**) Transmission setup of graded index waveguide for label-free sensing of biomolecules; (**b**) schematic of guided mode resonance; (**c**) two-channel microfluidic chip with embedded waveguide; (**d**) transmission intensity distribution on a charged coupled device; (**e**) intensity distribution along a specific row. Reproduced from [43] with permission, under CC 4.0, https://creativecommons.org/licenses/by/4.0/, (accessed on 7 September 2024); (**f**) MZI-based slot waveguide for refractive index biosensing. Reproduced with permission [44], under CC 4.0, https://creativecommons.org/licenses/by/4.0/, (accessed on 7 September 2024). GWT-GMR: gradient waveguide thickness—guided mode resonance, BCB: benzocyclobutene.

2.2.2. Luminescent Sensors

Luminescent-based optical sensors utilize the emission of light from luminescent materials in response to specific stimuli, making them highly effective for various biomedical applications like real-time monitoring of physiological parameters, sensing of metabolites, tissue engineering, and regeneration [46–48]. These sensors are primarily composed of four components: the luminescent material (e.g., fluorophores, nanoparticles, quantum dots, etc.), the optical transducer (OF or waveguide), the excitation source (typically laser or LED), and the detection system (e.g., photodiodes or CCD cameras). The choice of the luminescent material determines the sensor's sensitivity, stability, and specificity [49]. Three key requirements that luminescent sensors should meet are high selectivity, photostability, and sensitivity [50]. The intensity and lifetime of emission can be modulated by the interaction between the analyte-sensitive layer and the target analyte. Polymers contribute significantly to these aspects by enabling functionalization with specific recognition elements and protecting luminescent materials from environmental degradation. A notable category within these sensors is bioluminescence-based sensors, which emit light through biological organisms. The light production in these sensors is driven by the biochemical oxidation of the fluorophore molecule (e.g., luciferin). This sensing mechanism, known as bioluminescence resonance energy transfer, does not require external excitation. Bioluminescence-based sensors are versatile and can be utilized for detecting biomolecules, monitoring cellular processes, imaging tissues, conducting fluorescence thermometry, and facilitating point-of-care diagnostics [49,51,52]. Polymeric materials enable advanced fab-

rication techniques such as the layer-by-layer (LbL) nano-assembly, which allows for the creation of luminescent sensors with tailored properties [50]. By incorporating luminescent materials within polymer layers, sensors achieve enhanced sensitivity and specificity for target analytes. A difunctional hydrogel optical fiber-based luminescence sensor has been demonstrated for simultaneous glucose (0–20 mM) and pH (5.4–7.8) monitoring. Fluorescein derivatives were utilized for pH sensing and CdTe QDs for glucose sensing, while the hydrogel matrix served as a biocompatible, flexible matrix that encapsulates fluorescent materials and QDs, providing a stable environment for proper functioning [53]. Luminescent-based PDMS OFs containing lanthanide-based upconversion nanoparticles (UCNP) have also been utilized as a wearable multifunctional sensor for simultaneous real-time monitoring of skin temperature and mechanical motions of the human body, as depicted in Figure 4 [54]. The polymer matrix provides the necessary flexibility and stretchability, making the sensor suitable for wearable applications.

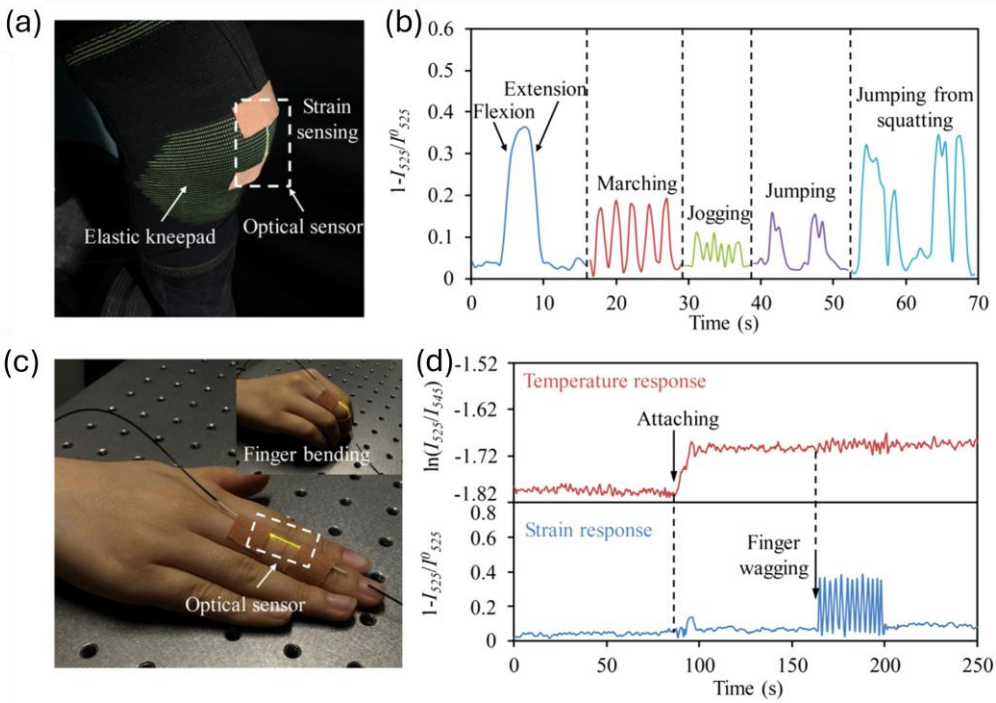

Figure 4. (**a**) Stretchable and multifunctional optical sensor integrated with knee pad to monitor knee-related motions; (**b**) strain response recorded by optical sensor for various knee motions; (**c**) sensor attached to finger for simultaneous detection of motion and skin temperature; (**d**) temperature and strain response of sensor during finger wagging. Reprinted with permission from [54] © Optical Society of America.

2.2.3. Surface Plasmon Resonance Sensors

The SPR technique relies on the excitation of surface plasmon polaritons (SPPs), which are collective oscillations of free electrons at a metal-dielectric interface. The interaction of light at a specific angle and wavelength at this interface can resonantly excite SPPs. This makes them absorb light and generate an evanescent field with a penetration depth of a few hundred nm, which is highly sensitive to refractive index near the surface. The resonance condition for SPR depends on various parameters such as the wavelength of light, the metal's dielectric properties, and the material's refractive index adjacent to the metal surface [55]. Any changes in this refractive index, such as those caused by the binding of biomolecules to the metal surface, lead to a shift in the SPR angle or wavelength as shown in Figure 5a. This makes SPR an excellent technique for label-free, real-time detection of biomolecular interactions. PSPR (propagating surface plasmon resonance) and LSPR (localized surface plasmon resonance) are the two main types of SPR sensors. PSPR sensors are more sensitive and have a higher figure of merit, but

they are more complex and expensive. LSPR sensors are more straightforward, cost-effective, and suitable for measuring local refractive index changes [51]. SPR sensors are predominantly used for studying protein–protein, protein–small molecule, and protein–DNA interactions, detecting biomarkers (e.g., early-stage cancer diagnosis) and pathogens for disease diagnosis, developing lab-on-chip, point-of-care devices, studying drug-target interactions, and monitoring cell surface interactions and cell-based assays [55–58]. Recent studies have developed novel SPR sensors using liquid-core POF for refractive index detection in the range of 1.325–1.35 with a sensitivity of 16,750 nm/RIU. The liquid core and polytetrafluoroethylene cladding confine light and provide optical guidance while generating evanescent waves when the RI of the liquid core is ~1.33. Two side air holes in the cladding with a thin silver film are used for optimizing mode coupling [59]. A D-shaped perfluorinated OF with a 50 nm thick gold coating demonstrated a high refractive index sensitivity of 30,049.61 nm/RIU (26.5 times more than traditional SMF-SPR) for detecting human immunoglobulin G (IgG) as low as 245.4 ng/mL [60]. Another study utilized a D-shaped polymer optical fiber-based SPR methodology to create an Aptasensor with a polyethylene glycol (PEG) functional interface for the detection of thrombin, a key marker in blood coagulation. The sensor had an enhanced sensitivity of 0.14 nm/nM and a ~1 nM detection limit, making it useful for monitoring blood clotting disorders [61]. An additional study showcased a biosensor chip made from PMMA, which forms the planar optical waveguide structures crucial for guiding light and enabling the SPR sensing mechanism to detect 25-hydroxyvitamin D (OHD) in human serum. The sensor integrates a microfluidic chip and a two-channel SPR sensing scheme, with aptamers for vitamin D immobilized on the sensor surface as demonstrated in Figure 5b. It achieves a sensitivity of −0.752 pixel/nM for 25OHD concentrations from 0–100 nM. Designed for smartphone integration, this biosensor enables portable and point-of-care testing, making it valuable for healthcare diagnostics [62]. These advancements highlight the potential of polymer-based SPR sensors in enhancing sensitivity, reducing costs, and expanding applications in biomedical sensing.

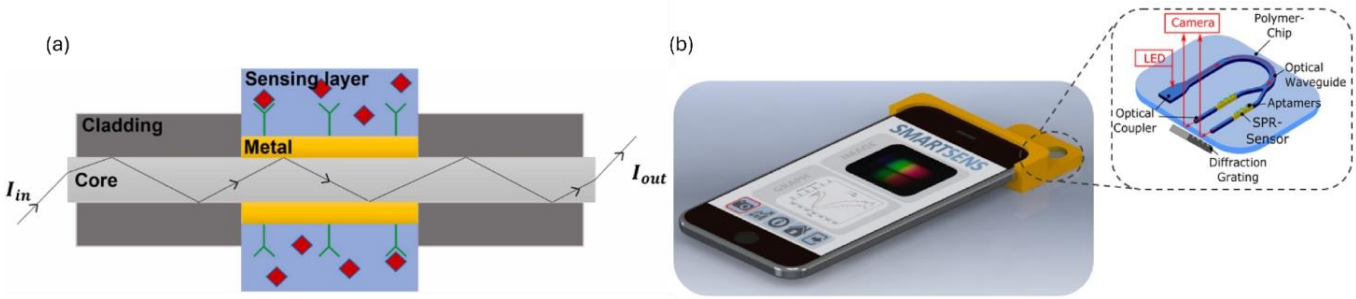

Figure 5. (**a**) Basic working principle of SPR sensor; (**b**) SPR-based planar optical smartphone-assisted bio-chip sensor for lab-on-chip applications. Reprinted from [55] and [62], respectively, under CC 4.0, https://creativecommons.org/licenses/by/4.0/, (accessed on 7 September 2024). I_{in}: Input light intensity launched into fiber optical fiber core, I_{out}: Output light intensity from optical fiber.

2.2.4. Polymer Optical Fiber Sensors

Polymer optical fibers are crafted from polymers such as PMMA, PS, and PDMS, which are well-regarded for their flexibility, ease of handling, and cost-effectiveness. Structurally, POFs feature a core and cladding configuration akin to silica OFs but offer distinct advantages. These advantages include higher yield strain (ranging from 1–6% on average), larger strain limits, i.e., elongation at break (can be 100% or more for polymers like PDMS), lower elastic modulus (spanning from a few MPa to GPa), tunability in refractive index contrast of core and cladding materials, hygroscopicity, higher thermal expansion, and thermo-optic coefficients. These mechanical and optical properties, detailed in Table 1 and Table 2, respectively, enhance the sensitivity of POF to various measures such as strain, pressure, refractive index, relative humidity, temperature, and force [1,11,13,18]. Additionally, POFs

such as PDMS, polyimide, PMMA, poly(vinyl alcohol) (PVA), and polyurethane exhibit inherent sensitivity to humidity and are biocompatible, making them particularly suitable for biomedical applications, such as medical implants and wearable health monitoring devices [20,63]. Furthermore, they provide a well-controlled and tunable refractive index, crucial for precise control in optical sensing and communication applications. Certain POFs, such as polyimide, also demonstrate resistance to high temperatures and chemicals, ensuring mechanical stability across diverse environments, which is essential for reliable performance in industrial and environmental monitoring. POF's environmentally friendly fabrication techniques add to their appeal, aligning with the growing emphasis on sustainable practices [19]. These properties collectively make POFs a versatile and robust choice for a wide range of sensing and biomedical applications. However, POFs also present several challenges that must be addressed to ensure their effective and practical use. One significant issue is their inherent sensitivity to humidity, which necessitates meticulous handling and packaging to avoid cross-sensitivity in applications involving the detection of other parameters. Additionally, coupling POFs of different diameters can be problematic, often resulting in inefficient light transmission. Their relatively low thermal threshold limits their use in high-temperature environments (>150 °C) due to their lower glass transition temperature than silica OFs, except polyimide, which can withstand temperatures of about 300 °C. Another challenge is related to distributed sensing, where the inherent attenuation of POFs can reduce their effectiveness over longer distances. Since POFs are viscoelastic materials, the stress–strain relationship varies with the strain rate, leading to potential sources of hysteresis and non-linearities. This viscoelastic nature can cause issues under cyclic loading, affecting the accuracy and reliability of the sensors over time. To mitigate these effects, it is crucial to compensate for the viscoelastic response through appropriate calibration and signal processing techniques. Understanding and addressing these challenges is essential to fully harnessing the potential of POFs in various sensing applications [13,64–66].

POF sensors operate based on the principle of light transmission through the fiber, where changes in the optical properties of the fiber (intensity, wavelength, phase, or polarization) are correlated with the parameter being measured.

Intensity-based POF sensors detect variations in the transmitted light intensity due to perturbations from external stimuli, such as bending, pressure, and surrounding refractive index variations. These types of sensors are favored for their straightforward detection mechanism (light source and photodetector) and cost-effectiveness. A few configurations are intensity-based sensors such as direct coupling, differential coupling, and microbending, are depicted in Figure 6(1a–1c). However, they are susceptible to fluctuations in the light source power, which can affect the accuracy and reliability of the measurements. Enhancements in light source stabilization and advanced signal processing can help mitigate some of these challenges [67,68]. These types of sensors have been used for glucose monitoring of interstitial fluids, blood oxygenation sensing, arterial pressure measurements, and wearable motion sensing, especially for gait and joint analysis [29,36,69,70].

Wavelength-based POF sensors, like fiber Bragg grating (FBG) sensors shown in Figure 6(2a,2b), measure shifts in the reflected peak wavelength caused by strain, temperature, or refractive index changes. Since the information is wavelength encoded, they do not suffer from light source power fluctuations and have better SNR than intensity-based sensors. The precise wavelength shifts allow for accurate and stable measurements, making them suitable for high-precision applications. However, FBG interrogation systems are necessary for wavelength demodulation, which can add complexity and cost to the setup [1,68]. A comprehensive account of this type of sensor, including their prevalent biomedical applications, is presented in the following sections.

Phase/polarization-based POF sensors analyze changes in the phase or polarization of light to detect subtle environmental variations with high precision. These sensors utilize interferometric techniques involving Mach–Zehnder, Fabry–Perot, Sagnac, and Michelson interferometers for various sensing applications requiring high accuracy and sensitivity

as shown in Figure 6(3a–3d). While these sensors offer exceptional performance, they require complex demodulation techniques, leading to higher costs and more sophisticated setups [1]. Typically these sensors are used for label-free biosensing applications involving point-of-care diagnostics (e.g., influenza A and breast cancer cells), detection of biomarkers and biomolecules (biotin–streptavidin), and lab on chip platforms [44,71–73].

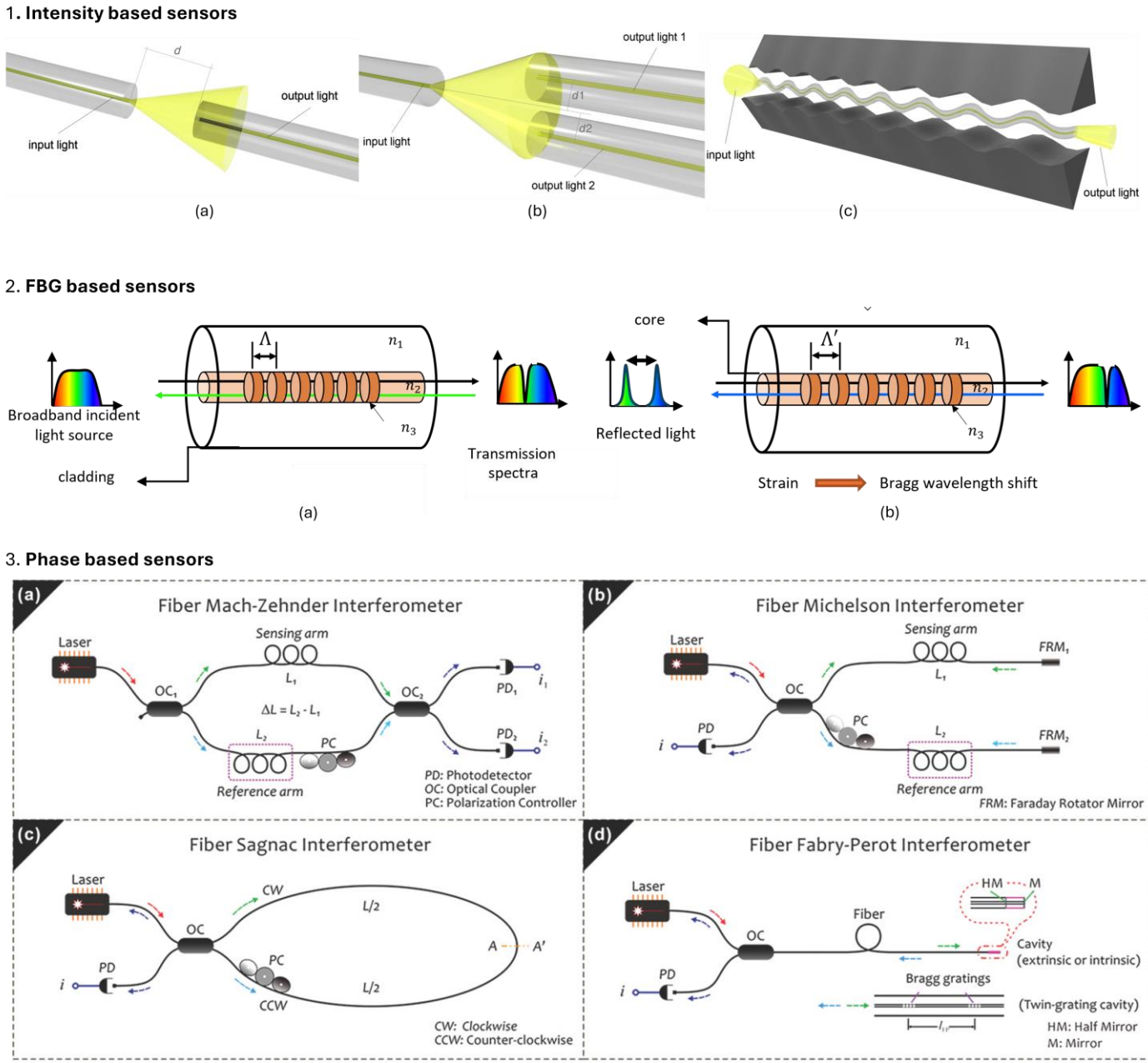

Figure 6. Various configurations of optical fiber sensors **1**. Intensity-based optical sensors; (**a**) represent simple design for monitoring transmitted light depending on distance d. (**b**) Transmitted light coupling can be enhanced using differential setup; (**c**) micro-bend sensing. Reprinted from [74], under CC 4.0, https://creativecommons.org/licenses/by/4.0/, (accessed on 7 September 2024);. **2.** FBG-based sensing, before (**a**) and after (**b**) changes in effective refractive index (n_{eff}) and grating period (Λ) due to external perturbations from various measurands. **3**. Phase-based sensing; (**a**) Mach–Zehnder, (**b**) Michelson, (**c**) Sagnac, and (**d**) Fabry–Perot interferometers. Reprinted from [75], under CC 3.0, https://creativecommons.org/licenses/by/3.0/, (accessed on 7 September 2024).

2.3. Point, Quasi-Distributed and Distributed Polymer-Based Optical Sensing

Polymer FBGs (PFBGs) primarily function as localized single-point sensors, but due to their multiplexing capabilities, they are also employed for quasi-distributed sensing. This enables comprehensive monitoring of various parameters over an extended area with high spatial resolution. FBGs consist of periodic variations in the refractive index along the core of an OF. These periodic changes reflect specific wavelengths of light while allowing others to pass through, forming a narrowband reflection spectrum centered around the Bragg wavelength, λ_B. Consequently, FBGs function as wavelength-selective filters coupling forward propagating mode to backward propagating mode due to periodic perturbations in the core of OF. Inscription of gratings in polymers is typically carried out using 248 nm KrF laser [76].

$$\lambda_B = 2n_{eff}\Lambda \tag{1}$$

$$\Delta\lambda_B = \lambda_B\left[\left(1-p_e\right)\varepsilon_z+(\alpha+\zeta)\,\Delta T\right] \tag{2}$$

where n_{eff} is the effective refractive index of the core, Λ is the grating period, ζ is thermo-optic coefficient ($\frac{\partial n}{n\partial T}$), α is thermal expansion coefficient ($\frac{\partial \Lambda}{\Lambda\partial T}$), p_e represents strain-optic coefficient ($\frac{n^2}{2}(p_{12}-\upsilon(p_{11}+p_{12}))$, n is the refractive index of core, ε_z is the longitudinal strain applied along the propagation axis of OF, p_{11} and p_{12} are components of strain-optic tensor, and υ is the Poisson's ratio of fiber core.

PFBGs are inherently sensitive to strain, temperature, and humidity. Variations in these parameters alter Λ or n_{eff} resulting in a Bragg wavelength shift (Equation (1)). The shift is due to changes in thermo-optic ($\zeta = \frac{\partial n}{n\partial T}$), thermal expansion ($\alpha = \frac{\partial \Lambda}{\Lambda\partial T}$), and strain-optic coefficients $\left(p_e\right)$. Any measurement that can reflect changes in either strain or temperature can be detected using FBGs by monitoring Bragg wavelength shifts. PFBGs exhibit significantly higher strain and temperature sensitivities compared to standard silica FBGs [1,76]. Specifically, PFBGs based on PMMA and CYTOP demonstrate strain sensitivities from 1.39 to 5.15 pm/$\mu\varepsilon$, temperature sensitivities between 18 and -74 pm/°C, and humidity sensitivity ranging from 0.3–11.7 pm/%RH at Bragg wavelengths ranging from 1530–1580 nm, in contrast to typical silica FBGs, which are 1.2 pm/$\mu\varepsilon$ 10 pm/°C and 1.3 pm/%RH at 1550 nm. The higher strain sensitivity of PFBGs is attributed to lower Young's modulus polymers (e.g., PMMA 3.3 GPa, CYTOP 1.3 GPa compared to 73 GPa of silica). Additionally, their enhanced temperature sensitivity is due to larger thermal expansion coefficients (e.g., CYTOP polymer—7.4 $\times$ 10^{-5}/°C vs. silica—0.55 $\times$ 10^{-6}/°C) and thermo-optic coefficients (e.g., CYTOP polymer—-5.0 $\times$ 10^{-5}/°C vs. silica—8.6 $\times$ 10^{-6}/°C) [77–79]. Writing PFBGs under pre-strained conditions can further enhance and tune these sensitivities. Unlike standard FBGs, which have both positive thermal expansion and thermo-optic coefficients, CYTOP polymer features a positive thermal expansion coefficient and a negative thermo-optic coefficient. This unique combination allows PFBGs to exhibit a positive temperature sensitivity (18.2 pm/°C) when the fiber freely expands and a negative sensitivity (-69.5 pm/°C) when pre-strain restricts thermal expansion. This tunability and enhanced sensitivity make PFBGs particularly suitable for applications requiring precise strain and temperature measurements. However, as mentioned earlier in the introduction section, unlike silica FBGs, the sensitivities of PFBG sensors can vary slightly throughout the complete measurement cycle, depending on the specific parameter being detected. Temperature and humidity of unstrained and pre-strained CYTOP FBGs are depicted in Table 3 during their respective sensing cycles [79].

Table 3. Temperature and humidity sensitivities of silica and CYTOP FBGs during their respective measurement cycles. Reproduced from [79], under CC 4.0, https://creativecommons.org/licenses/by/4.0/, (accessed on 7 September 2024).

FBG Sensor Type	Increasing Temperature (pm/°C)	Decreasing Temperature (pm/°C)	Increasing Humidity (pm/%RH)	Decreasing Humidity (pm/%RH)
Silica (0% pre-strain)	12.6 ± 0.2	12.6 ± 0.2	1.3 ± 0.2	1.3 ± 0.2
CYTOP (0% pre-strain)	21.5 ± 0.3	18.0 ± 0.1	11.7 ± 0.2	11.0 ± 0.3
CYTOP (0.5% pre-strain)	−70.0 ± 1.4	−73.6 ± 1.6	0.7 ± 0.2	0.3 ± 0.2

Apart from these standard FBGs, various types of FBGs, such as etched, tapered, long-period, tilted, chirped, and phase-shifted polymer-based FBGs, have been explored for various healthcare sensing applications. Figure 7 showcases various FBG types and their typical spectra along with standard interrogation techniques involving source - detector combination of either rapid scanning tunable laser and photodetector or a broadband source (e.g., Superluminescent LED and a spectrometer).

Etched FBGs are specialized OFs in which cladding (sometimes core) is partially removed through chemical etching. This reduction in diameter changes material's mechanical properties. For example, a reduction in Young's modulus leads to an increase in thermal expansion coefficient and Poisson's ratio of POF, which enhances its sensitivity to temperature, strain, pressure, and especially to refractive index in the vicinity of FBGs. In contrast, standard FBGs are less suited for this type of sensing as core and cladding modes are well protected from the surrounding environment. The penetration depth of the evanescent field ranges from 50 nm–1000 nm depending on factors such as angle of incidence, refractive indices, and wavelength, thus limiting their interaction with external stimuli [80]. This penetration depth is far smaller than the cladding diameter (typically 125 µm), resulting in no interaction between the optical signal and external refractive index perturbation. After reducing the cladding thickness, the evanescent field extends (to several µm) into the external environment [81], resulting in a more significant Bragg wavelength shift in response to external stimuli. These FBGs have been utilized as blood pressure transducers for monitoring blood pressure, measuring human breathing rate, and foot pressure sensors [82,83].

Long-period gratings (LPGs) have longer grating periods (100 µm–1 mm) compared to standard FBGs (hundreds of nm). LPGs couple core-guided light into cladding modes at specific wavelengths, which are determined by the grating period and the effective refractive indices of the core and cladding modes. Changes in the surrounding medium interact with an evanescent wave of cladding modes, which in turn changes the resonance of cladding modes. Maximum sensitivity occurs when the grating length is chosen so that coupling to cladding modes happens at the phase-matching turning point. Since resonance wavelengths are inherently sensitive to changes in the surrounding refractive index and thickness of nanoscale coatings deposited on cladding, they are ideal for use as refractometers and biosensors [80,84,85].

Tilted FBGs have refractive index modulation that is slightly angled with respect to the propagation axis. The grating period is typically around 500 nm. The tilt enhances the interaction between the core and cladding modes, leading to the coupling between the forward propagating core mode to counter-propagating core mode and between the forward propagating core mode to counter-propagating cladding modes. The cladding mode evanescent wave interacts with a surrounding medium, which changes the effective refractive index and thus changes the wavelengths of the cladding mode coupling features. Normally, these do not require etching, and therefore, the integrity of OF remains intact. TFBGs can also be used for simultaneous multiparameter measurements since the core and cladding modes have the same temperature but different strain sensitivity. They are usually used for biochemical sensing [86].

Chirped FBGs have a refractive index modulation period that varies along the propagation axis of OF, resulting in a chirped grating structure. This chirp causes different

wavelengths of light to be reflected from various positions along the grating, resulting in a broadband spectrum instead of a single wavelength. Also, each section of the grating is dependent on strain and temperature. They have been employed for RF thermal and laser ablation monitoring to monitor temperature profiles in tissue. PMMA-based CFBGs have been demonstrated to detect spatially non-uniform temperature profiles with a temperature sensitivity of −191.4 pm/°C for minimally invasive biomedical treatments [76,87,88].

Pi-phase shifted FBGs have π-phase jump introduced at the center of the grating. This phase shift disrupts the periodic structure, creating a localized defect mode, seemingly acting as a Fabry–Perot cavity. It can be visualized as two FBGs forming a Fabry–Perot cavity with only one resonance state. This creates a narrow transmission peak (10—50 pm) within a broader reflection spectrum (0.2—0.5 nm), which significantly enhances the sensitivity and resolution of the grating. The sensitivity of the π-phase shifted FBGs is further enhanced in polymer fibers due to the polymer's higher thermo-optic and strain-optic coefficients compared to silica. In a study, pi-phase FBGs were written at 850 nm on PMMA-based microstructured POF. It showcased pressure, temperature, and humidity sensitivities of 0.46 ± 0.03 pm/kPa, −57 ± 1 pm/°C, and 19.9 ± 2.5 pm/%RH in the range of 0–400 kPa, 22–52 °C, and 30–90%RH, respectively [89–91].

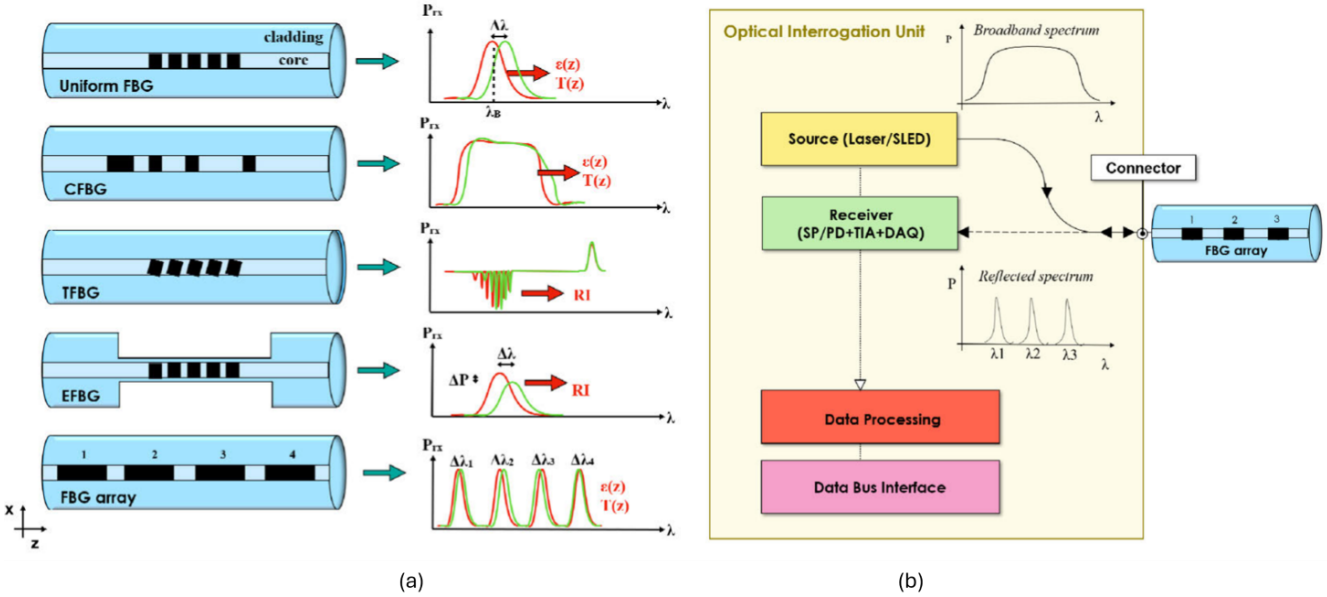

Figure 7. Various configurations of FBGs and their spectral responses. (**a**) Uniform, chirped, tilted, etched, and array FBGs. (**b**) Standard interrogation unit for FBGs (either SLED source coupled to a interrogator or a tunable laser source coupled to a photodetector). Reproduced from [92], under CC 4.0, https://creativecommons.org/licenses/by/4.0/, (accessed on 7 September 2024). CFBG: chirped FBG, TFBG: tilted FBG, EFBG: etched FBG, ε: strain, T: temperature, RI: refractive index, SLED: superluminescent LED, SP: spectrometer, PD: phototdetector, TIA: transimpedance amplifier, DAQ: data acquisition system.

In addition to quasi-distributed sensors, distributed optical fiber sensors (DOFS) leverage the optical properties of OFs to monitor various changes in parameters along the entire length of OF. DOFS relies on analyzing the backscattered (typically) or transmitted light within the OF to obtain spatially resolved measurements along the entire length of the fiber. The primary mechanisms underlying DOFS involve different types of light scattering within the fiber, namely Rayleigh, Brillouin, and Raman scattering. Each type of scattering provides different information and is utilized in various kinds of distributed sensing systems [7,93,94]. Rayleigh backscattering is caused by density and composition fluctuations in the OF material. It is generally used to provide information about fiber's attenuation and can be used to detect breaks or heterogeneities of fiber. Techniques such as optical time domain reflectometry and optical frequency domain reflectometry measure

the time and frequency domain variations of the scattered light along the fiber. Brillouin scattering arises from the interaction between the light wave and acoustic phonons in the fiber, leading to frequency shifts in the scattered light. Brillouin-based sensors are effective for detailed temperature and strain sensing, utilizing methods like Brillouin optical time domain analysis and Brillouin optical frequency domain analysis (BOFDA). Raman scattering is caused by the inelastic scattering of light, where incident photons interact with molecular vibrations, leading to energy shifts in the scattered photons. Raman-based DOFS is primarily used for temperature sensing through distributed temperature sensing systems, which leverage the temperature-dependent shifts in Raman-backscattered light to provide precise temperature profiles.

Below are examples of polymer-based biomedical sensing applications utilizing various optical sensor configurations previously discussed in this section. G.T. Kanellos et al. reported a 2D pressure sensor for potential applications in human skin pressure measurements, wearable sensors, hospital bed monitoring, and wheelchair seating sensors. The sensor configuration includes an FBG array embedded in a 2 × 2 cm^2 PDMS sheet having a 2.5 mm thickness and spatial resolution of 1 × 1 cm^2 [95]. S. Korganbayev et al. utilized chirped FBGs inscribed on PMMA microstructured POF for monitoring temperature profile (temperature sensitivity of −191.4 pm/°C) during thermal minimally invasive treatments [87]. A.G. Leal-Junior et al. presented a multiplexed POF intensity-based sensor for multiparameter measurements, including 3-DOF angle measurements [96]. Z. Katrenova et al. demonstrated a 2D distributed pressure sensor that can be utilized for force and strain mapping during prosthetic treatment and human bite force measurements. The configuration involved standard SMF fiber embedded inside silicone material with a pressure sensitivity of ~0.05 pm/mmHg and a sensing area of 2 × 6 cm^2 [97]. The embedded five FBG array was utilized for prosthetic knee joint pressure mapping with PMMA coating by L. Mohanty et al. [98]. Y. Mizuno et al. reported POF (PMMA and perfluorinated graded-index polymer) for distributed strain and temperature sensing based on Brillouin scattering [99]. In another study, J. Witt et al. demonstrated an MRI-compatible respiration sensor based on POF—OTDR and macrobending optical technology embedded in medical textiles that can sense elongation up to 3%. PMMA step index fiber of 500 µm with macrobends was stitched on elastic textile, which on elongation changes the bending radius of OF, thereby changing OF attenuation and thus OTDR back scattered light for continuous measurement of abdominal respiratory movement [94].

2.4. Polymer-Coated Optical Fibers

A polymer-coated optical fiber (PCOF) consists of a standard OF coated with single or multiple polymer coatings. These fibers leverage the unique properties of polymeric materials to enhance the functionality and biocompatibility of OF for biomedical sensing applications. The polymer coating, typically made from polyimide, silicone, or acrylates, serves multiple purposes. It provides a protective layer that improves the mechanical strength, flexibility, and durability of the underlying OF, enabling it to withstand the rigors of biomedical environments [100]. Additionally, the polymer coating can be engineered to exhibit specific enhancements in sensing capabilities, such as responsiveness to changes in temperature, strain, pressure, refractive index, or the presence of target analytes, thereby acting as a transducer [101,102]. This is achieved by incorporating functional groups, dopants, or molecularly imprinted polymers into the coating material [103]. The sensing mechanism in PCOF relies on the modulation of the fiber's optical properties, such as intensity, wavelength, phase, or polarization, in response to the measured parameter, as described above. These changes correlate to the target parameter, allowing the fiber to function as a sensor. The same fiber material can give diverse sensing responses when used with different coatings. Thus, providing flexibility in choosing customized fiber and coating material for specific applications. For instance, during temperature sensing applications, specific polymeric materials such as PDMS are chosen since they have higher thermal expansion (300×10^{-6}/°C) and thermo-optic coefficients (-4.66×10^{-4}/°C) compared to silica glass,

improving the temperature sensitivity of micro-fibers to 3101.8 pm/°C compared to that of silica OF 10 pm/°C [104]. Z. Liu et al. showcased enhancement in temperature sensitivity (−41.58 pm/°C) due to the PDMS coating acting as a temperature transducer on one arm of a knot microfiber resonator-based M-Z interferometer for independent temperature sensor probe application [105]. P. Rivero et al. showcased the development of a highly sensitive optical sensor for respiratory monitoring, with humidity sensitivity of 0.455 nm/%RH and response times of 692 ms and 839 ms for rise/fall, respectively, utilizing a polymer matrix embedded with silver nanoparticles. The polymer matrix, polyelectrolyte poly(allylamine hydrochloride) and polyelectrolyte poly(acrylic acid, sodium salt), serves as a flexible platform that supports the integration of silver nanoparticles, which enhance the sensor's sensitivity due to its unique plasmonic properties. This setup leverages the lossy mode resonance (LMR) phenomenon, where light attenuation within the OF varies with changes in the surrounding refractive index. Changes in humidity, caused by breathing, alter the refractive index of the polymer matrix, leading to shifts in the LMR wavelength [106]. B. Zhaou et al. reported the first biocompatible hydrogel-coated silica multimode OF probe for real-time, in vivo monitoring of minute pH changes in the brains of moving mice. The pH sensor has a dynamic range of 3.0–9.0 and a resolution of 0.0014 pH units. The basic principle involves the hydrogel coating, which is sensitive to pH changes. When the pH changes, the fluorescence properties of the embedded microspheres change, which is detected by the fiber-optic probe. In vivo tests disclosed that during cerebral ischemia, the pH in the brain decreased by about 0.5 units after approximately 15 min, and during epileptic seizures, the pH in the hippocampus decreased by about 0.3 units after around 1 h [107]. In another study, T. Dey explored LPG enhancement for biosensing. The principle involves operating near the mode transition and turn-around point of cladding modes, reducing the cladding diameter (down to 85 μm), and increasing the order number of cladding modes to boost sensitivity. A polymer coating of poly(allylamine hydrochloride) and poly(sodium 4-styrenesulfonate) with a total thickness of 266 nm is further applied to etched LPG to further enhance sensitivity. The biosensor was tested with an IgG/anti-IgG immunoassay in human serum, demonstrating its effectiveness with detection limits as low as 6.9×10^{-8} μg/mL [108]. For strain sensing applications, especially with standard FBGs, specific polymeric coating materials are chosen to have a higher Poisson's ratio and a lower Young's modulus, along with lower thermal expansion, and thermo-optic coefficients are selected to amplify Bragg wavelengths due to strain and reduced cross-sensitivity. W. Zhang et al. demonstrated the use of microstructured OF for potential high-resolution manometry applications using a homogeneous silicone coating of 3 mm, leading to an increase in pressure sensitivity to 2.2 nm/MPa compared to 3.04 pm/MPa for typical gratings [109,110].

The versatility of PCOFs enables their use in a wide range of biomedical sensing applications, including vital sign monitoring (e.g., tissue oxygenation), biochemical sensing (e.g., pH or ion concentration in bodily fluids), minimally invasive surgical tools, physiological pressure indices, and implantable and wearable devices [103,109,111,112]. The aforementioned polymer-based optical sensors can be assessed for their utility in biomedical applications based on key performance parameters such as sensitivity, specificity, response time, durability, resolution, biocompatibility, repeatability, limit of detection, and functional ability.

PCOF and POF have their distinct advantages and disadvantages. Typically, PCOFs have enhanced mechanical strength, low optical loss, stable transmission, and versatility in coatings and functional integration since polymers act only as active elements (transducer/amplifier) and/or passive elements (providing support and immobilization to the biochemical transducer), but optical transmission occurs via the silica core of OF. However, these advantages come at the expense of a complex fabrication process, uniformity issues, and adhesion challenges. POFs have inherent flexibility, elasticity, biocompatibility, ease of surface functionalization, and surface modifications but may have lower mechanical strength and high optical losses. Specific requirements of biomedical applications,

such as mechanical strength, flexibility, biocompatibility, optical performance, and ease of fabrication, decide the choice between them.

3. Polymer Material Selection

Polymer material selection is crucial for biomedical applications, as the choice of polymer directly impacts the device's performance, safety, chemical stability, and efficacy. In general, biomedical polymers must be biocompatible, as they should not elicit an adverse immune response or cause toxicity when in contact with biological systems [113]. Biodegradable and hydrophilic polymers are commonly used with implantable optical sensors for applications involving temporary implants, tissue engineering scaffolds, and drug delivery systems since these applications require materials that are non-toxic, non-reactive, with the ability to degrade inside biological tissues, and stable in bodily fluids. Wearable and soft robotics sensors benefit from elastomers and hydrophilic polymers, as characteristics like flexibility, durability, and moisture retention capabilities are needed for applications in physiological monitoring, minimally invasive surgery, and sweat analysis. Stimuli-responsive and biocompatible polymeric materials have been commonly used for invasive functional monitoring sensors such as pH and temperature monitoring (e.g., gastrointestinal monitoring or temperature-controlled drug delivery systems) since these polymers must respond predictably to specific stimuli and return to their initial state when the stimulus is removed. Conductive polymers (CPs) are regularly used for neural interface-related applications such as brain activity monitoring and neural prosthetics, as high electrical conductivity is needed to record and stimulate neural activity accurately. MIPs are instead used with biosensors to detect specific biomolecules involving the detection of pathogens, proteins, and drug delivery with controlled release, as MIPs provide the ability to create specific binding sites for target molecules, enhancing the sensitivity and selectivity of biosensors.

3.1. Biocompatible and Biodegradable Polymers

Biocompatible polymers are designed to be non-toxic, non-immunogenic, and non-carcinogenic. Examples include polyethylene glycol (PEG), PLA, polycaprolactone, PVA, and silk fibroin. These polymers are often used in drug delivery systems, tissue engineering scaffolds, and medical devices due to their excellent biocompatibility and ability to integrate with living tissues [2].

Biodegradable polymers are materials that can be broken down and removed from the body after they have served their function. These polymers are used in biomedical applications such as surgical sutures, implants, and tissue engineering scaffolds, where they must degrade at a controlled rate to match the healing process. Biodegradable polymers must possess specific properties, including biocompatibility, controlled degradation time, and mechanical strength, to ensure they do not evoke a sustained inflammatory response and produce non-toxic degradation products. Clinical applications of biocompatible and biodegradable POFs include but are not limited to biosensing, drug delivery, neural recording, and optogenetics [31]. For instance, genetically engineered silk fiber protein was used to manufacture optical waveguides for biocompatible and biodegradable implants for light-guiding efficiency, having optical loss of 0.8 dB/cm in air and 1.9 dB/cm in mouse muscles [114]. In a separate study, PLA-based comb-shape planar waveguides have been used for deep tissue treatments, which can potentially be also used for light delivery for sensing, as depicted in Figure 8(1). The degradation time of polymers could be controlled from weeks to months [115]. Citrate-based POF has been reported for fluorescence sensing and in vivo deep tissue light propagation with optical loss of 0.4 dB/cm, Figure 8(2) [39].

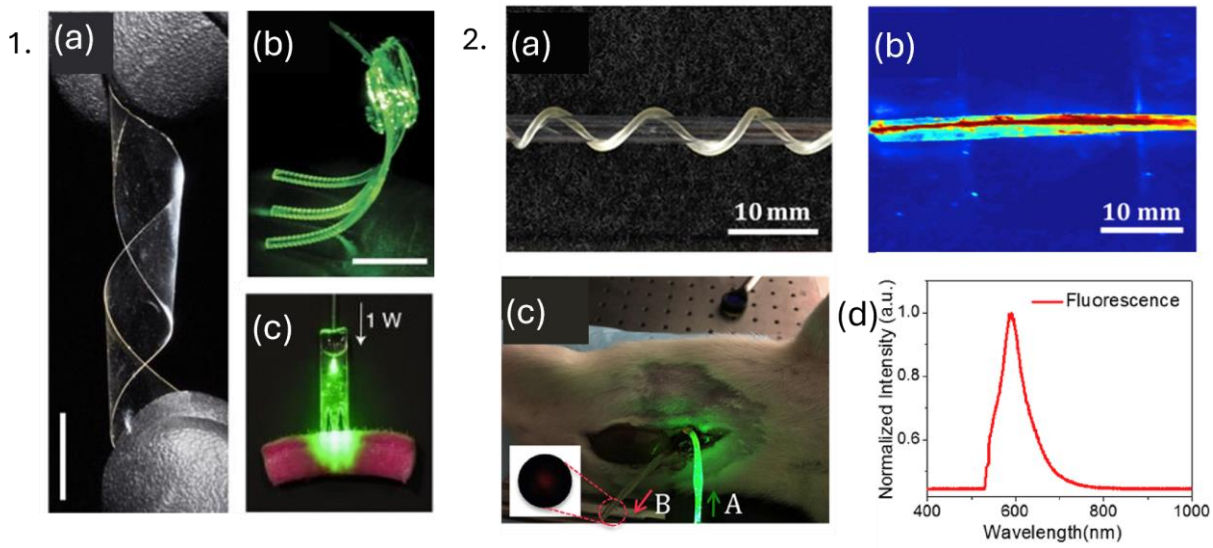

Figure 8. 1. (**a**) Poly(L-lactic acid) biopolymer film, (**b**) polyethylene glycol hydrogel waveguide array guiding green laser light, (**c**) biopolymer-based waveguide light delivery of photoactivated area at dyed porcine skin. Reprinted from [115], under CC 4.0 (https://creativecommons.org/licenses/by/4.0/), (accessed on 7 September 2024). **2**. (**a**) Citrate-based optical fiber twisted around glass, (**b**) light delivery using citrate-based fiber, (**c**) in vivo deep tissue fluorescence sensing using citrate-based fibers, (**d**) fluorescence spectrum acquired from light collection fiber (denoted as B in Figure 8(2c) inset). Reprinted with permission from [39].

3.2. Hydrophilic Polymers

Hydrophilic polymers, such as PVA, hydrogels, and PEG, are particularly useful in biomedical applications because they absorb and retain significant amounts of water, mimicking the properties of natural biological tissues. These polymers are advantageous in various medical biomaterials often used in contact lenses, wound dressings, and drug delivery systems. Hydrogels, in particular, can hold large amounts of water (water retaining capacity—76%) [116], providing a moist environment that promotes healing and facilitates the diffusion of therapeutic agents. This characteristic is vital in applications where sustained release of drugs is required, as it enhances bioavailability and therapeutic efficacy. Furthermore, hydrogel waveguides have emerged as promising platforms for intensity-based sensing applications like continuous glucose monitoring, metal-ion detection, and toxicity sensing, demonstrating their versatility and potential in real-time monitoring [11]. Another work reported OF consisting of poly(ethylene glycol) diacrylate (PEGDA) and polyacrylamide as core and alginate hydrogel as cladding for implantable glucose biosensor [29], as shown in Figure 9(1). The sensor operates as an intensity-based refractive index sensor, where increased glucose concentration leads to swelling of fiber, leading to a change in transmitted light, which is monitored by measuring attenuation relative to 532 nm input light. Figure 9(2) illustrates the reusability of the hydrogel fiber sensor, the dependence of the core refractive index of fiber on glucose concentration, transmitted light across hydrogel fiber, and sensor sensitivity (1.2 mmol L^{-1}). A.M. Shrivastav et al. reported microstructured optical fiber and chitosan film-based Fabry–Perot interferometer for real-time breath monitoring. Refractive index changes in chitosan polymer cause phase shifts in reflected light, leading to a shift in the interference pattern, which was observed to be 28 pm in this study. Stability, response, and analysis of the sensor showcased promising results for breath monitoring (Figure 9(3,4)) [117].

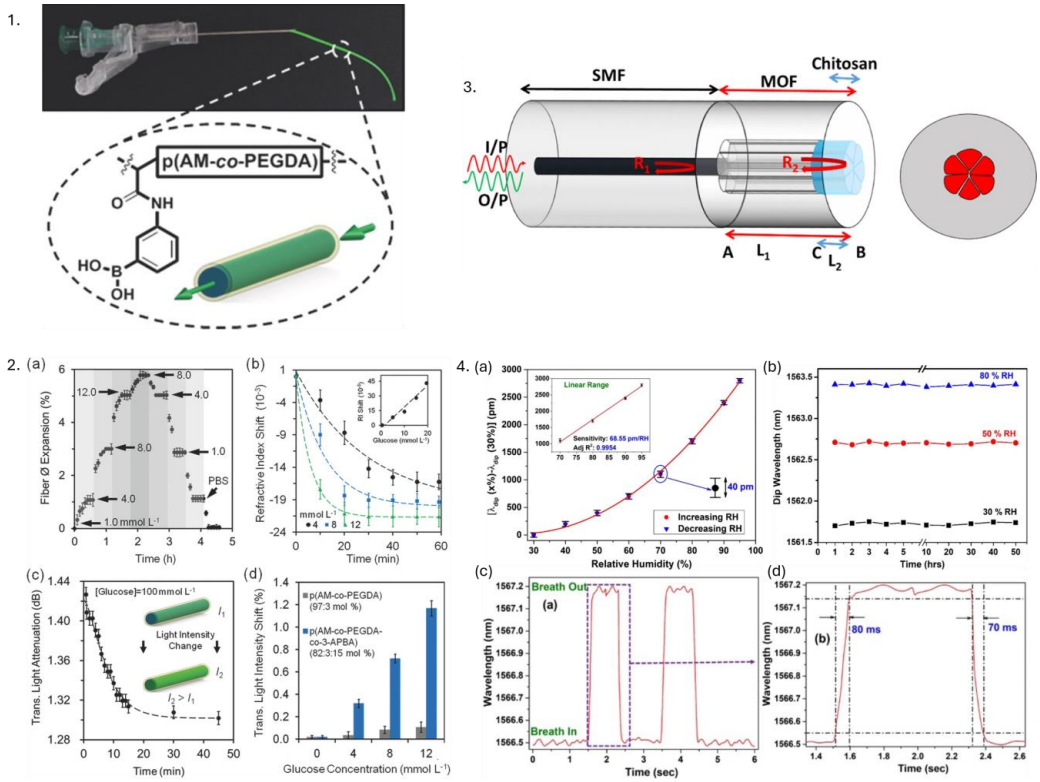

Figure 9. 1. Hydrogel fibers consisting of poly(acrylamide-co-poly(ethylene glycol) diacrylate) core with functionalized phenylboronic acid for continuous real-time glucose monitoring. **2**. p(AM-co-PEGDA-co-3-APBA) hydrogel fiber as glucose sensor. (**a**) Reusability of fiber—fiber expanded by 6% as the conc. of glucose increased from 1.0 to 12.0 mmolL^{-1} and decreased back to its initial value when conc. decreased. (**b**) Refractive index variation with respect to glucose conc. (**c**) Transmitted light attenuation across fiber as a function of time boronic acid–glucose cis diol binding. (**d**) Transmitted light intensity with respect to glucose concentration. Reprinted from [29], under CC 4.0, https://creativecommons.org/licenses/by/4.0/, (accessed on 7 September 2024). **3**. Microstructured optical fiber and chitosan film-based Fabry–Perot interferometer. 4. (**a**) Wavelength shift of specific dip of interference pattern with respect to humidity. (**b**) Stability of humidity sensor. (**c**) Response of the sensor to human breath containing two cycles of inhalation and exhalation. (**d**) Analysis of human breath on one cycle. Reprinted from [117], under CC 4.0, https://creativecommons.org/licenses/by/4.0/, (accessed on 7 September 2024).

The unique properties of hydrophilic polymers not only facilitate their integration into various biomedical applications but also pave the way for the development of novel sensing technologies that can significantly enhance patient care and monitoring [11,18]. Some disadvantages of hydrophilic-based optical sensors primarily arise due to material properties and environmental sensitivities. Polymers, such as hydrogels and chitosan, can degrade or swell over time, especially in harsh or high-humidity environments, which can impact their structural integrity and sensor accuracy. While they are biocompatible, these materials often lack the mechanical robustness required for long-term or high-stress applications, leading to potential mechanical failure. Regular calibration and signal drift over time can affect the accuracy of glucose-sensitive hydrogel optical fibers. Additionally, the hydrophilic nature of these materials makes them susceptible to biofouling.

3.3. Stimuli-Responsive Polymers

Stimuli-responsive polymers are “smart” materials capable of changing their properties (e.g., volumetric changes) in response to external stimuli, such as pH, temperature, light, or enzymes. These polymers are valuable in biomedical applications because they can

be designed to respond to specific biological cues such as detecting biomolecules (proteins, enzymes, glucose, and nucleic acids), enabling targeted drug delivery, controlled release, and tissue engineering. For instance, pH-sensitive hydrogel polymers can be employed for targeted drug delivery to tumors, while temperature-responsive polymers can be used for cell culture and tissue engineering. A notable example is a sensitive polymer like Poly(N-isopropylacrylamide), which undergoes a phase transition around its lower critical solution temperature (~32 °C), leading to a significant change in shape (either swelling or shrinking) [118]. Shu et al. used poly(N-isopropylacrylamide) (pNIPAm)-based microgels containing silver nanoparticles (AgNPs) for H_2O_2 sensing, which acts as a biomarker for neurodegeneration, cardiovascular diseases, and cancer [119]. Azobenzene-containing polymers undergo reversible trans–cis isomerization upon exposure to specific wavelengths of light, altering their optical properties, which can be used for controllable drug release systems and light-activated biosensors for localized therapy and diagnostics [120,121]. Shape memory polymers have been explored to create optical fibers such that they can be pre-programmed to have a specific shape. Various configurations of such OFs have been represented in Figure 10. Upon exposure to external stimuli, these fibers deform, and when heated around 80 °C, they return to their original programmed configuration. However, their shape retention ability decreases with repeated cycles; after 25 cycles, the fibers recover only 53% of their programmed angle. The sample of polyethylene terephthalate glycol as the core of an OF in particular maintained good optical performance and minimal transmission loss up to 18 cycles. This feature of adapting to complex environments can be particularly useful for endoscopy and flexible biomedical sensing applications [122]. In another study, an anti-biofouling and biocompatible zwitterionic poly-carboxybetaine (PCB) hydrogel is proposed to monitor pH and glucose level in in vivo diabetic wound treatment, specifically diabetic ulcers. A pH indicator dye, phenol red, and two glucose sensing enzymes, horseradish peroxidase and glucose oxidase, were encapsulated inside the PCB hydrogel matrix. The dye indicator showcased pH-sensitive color change (pH range: 4–8) in the vicinity of the wound environment, whereas glucose sensing enzymes catalyzed glucose oxidation, forming a dichlorofluorescein fluorescent product. The florescence signal and color change were monitored using a smartphone for precise measurements [123].

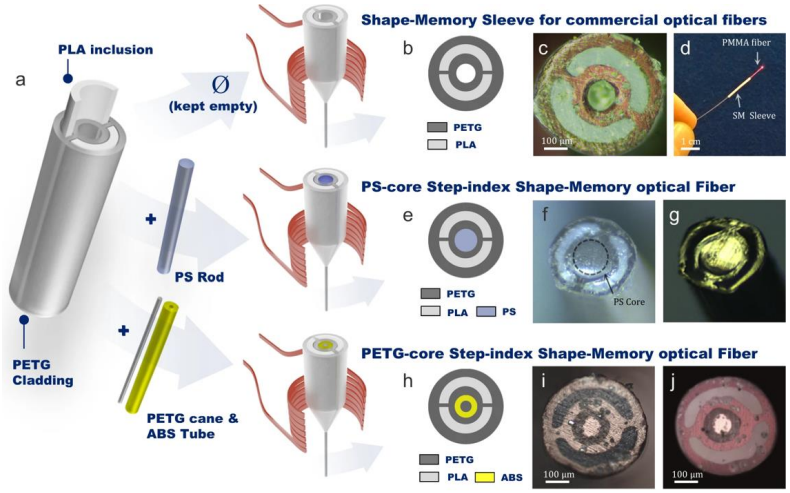

Figure 10. (**a**) Polylactic acid (PLA)/polyethylene terephthalate glycol (PETG) for shape-memory fiber with three configurations; empty central hole, filled with a polystyrene (PS) rod, and filled with acrylonitrile butadiene styrene (ABS); (**b**) represents diagram; and (**c**) cross-sectional optical image of hollow sleeve. (**d**) PMMA fiber integrated with a hollow sleeve. (**e**) Represents diagram and cross-sectional optical image in (**f**) reflection and (**g**) transmission of a PS optical fiber. (**h**) Diagram and cross-sectional optical image in (**i**) reflection and (**j**) transmission of a PETG optical fiber. Reproduced from [122], under CC 4.0, https://creativecommons.org/licenses/by/4.0/, (accessed on 7 September 2024).

3.4. Conductive Polymers

CPs have emerged as potential materials for biomedical applications ranging from biosensors, neural probes, bio-actuators, tissue engineering scaffolds, neural prostheses, and drug delivery devices. CPs are particularly attractive as they provide the possibility of chemical surface variation with physiologically active species for the enhancement of functionality and biocompatibility of electrodes [124]. The presence of conjugated double bonds in the main chain of CPs imparts conductivity by allowing π electrons to delocalize into a conduction band, potentially resulting in metallic behavior. However, bond alternation causes instability, leading to an energy gap in the electronic spectrum. To overcome this gap and enhance conductivity, dopant ions are introduced, carrying extra electrons to stabilize the oxidized polymer chain. When a potential is applied, ions move in or out of the CP film, facilitating charge transfer. CPs can be doped with both p-type and n-type dopants, using molecules such as small salt ions (e.g., Cl^-, Br^-, $NO_3{}^-$) and larger entities like hyaluronic acid, peptides, or polymers [124,125]. CPs such as polypyrrole (PPy), polyaniline, and poly(3,4-ethylenedioxythiophene) (PEDOT) modulate electrical and optical signals in response to external stimuli. For instance, PPy-coated optical fibers are employed in neural interfaces to monitor brain activity by detecting ionic changes, significantly altering the fiber's optical characteristics [126–128]. In another study, conductive polyethylene was used as a recording electrode for a multimodality fiber probe wherein light guidance was provided by the refractive index difference between the PC and a cyclic olefin copolymer for optical stimulation, neural recording, and drug delivery on mice [129]. In a different study, a miniature (diameter <200 μm and weighing 0.5 g) polymer integrated probe with six customized conductive polyethylene and two microfluidic channels was embedded inside the PC core, and cyclic olefin copolymer cladding was showcased for behavioral optogenetic studies of neural circuits in mice [130]. Another study utilized PEDOT polymer deposited on SMF-28 optical fiber via chemical vapor deposition with a thickness of 500 nm, which can be potentially used for biomedical sensing applications [127].

3.5. Elastomers

This class of polymer consists of long, coiled molecular chains that stretch and return to their original shape, making them ideal for dynamic environments. Elastomeric polymers, such as PDMS, polyurethane, and silicone rubber, are integral to the development of polymer-based optical sensors for biomedical applications due to their exceptional elasticity and resilience [11]. The optical and mechanical properties can be tuned by altering the mixing ratio of the base elastomer and curing agent along with the curing temperature. For instance, a novel stretchable optical temperature sensor was developed using UCNPs incorporated into PDMS optical fibers. The temperature sensitivity of the sensor was found to be 1.8%/°C in the range of 25–70 °C with a detection limit of ±0.3 °C. The step-index core-cladding structure of the PDMS fiber effectively excited the luminescent UCNPs, achieving a linear sensing range in the given temperature range through ratiometric measurements of dual-wavelength emissions under near-infrared excitation, thus demonstrating its potential by monitoring both interior and surface human body temperatures [3]. Figure 11 depicts the mechanical flexibility of the PDMS optical sensor, synthesized UCNP-loaded sights in the OF, cycling test of temperature sensing inside the incubator (26–50 °C), and response and recovery behavior of the PDMS temperature sensor. To et al. reported a gold-coated PDMS stretchable optical waveguide for wearable detection of human motions, allowing measurements of strain, pressure, and curvature based on changes in light transmission [131]. Meanwhile, Prata et al. demonstrated respiratory rate monitoring using polyurethane-embedded FBGs. Silicone rubber is employed in constructing sensors that mimic soft tissue properties, enhancing prosthetic and robotic applications. Silicone rubber-encapsulated FBGs are used to create flexible strain, temperature, and humidity sensors for non-invasive chest wall displacement and heart rate and respiratory frequency monitoring.

The unique mechanical properties of elastomeric polymers facilitate the creation of reliable, real-time monitoring devices for various physiological parameters [1,11].

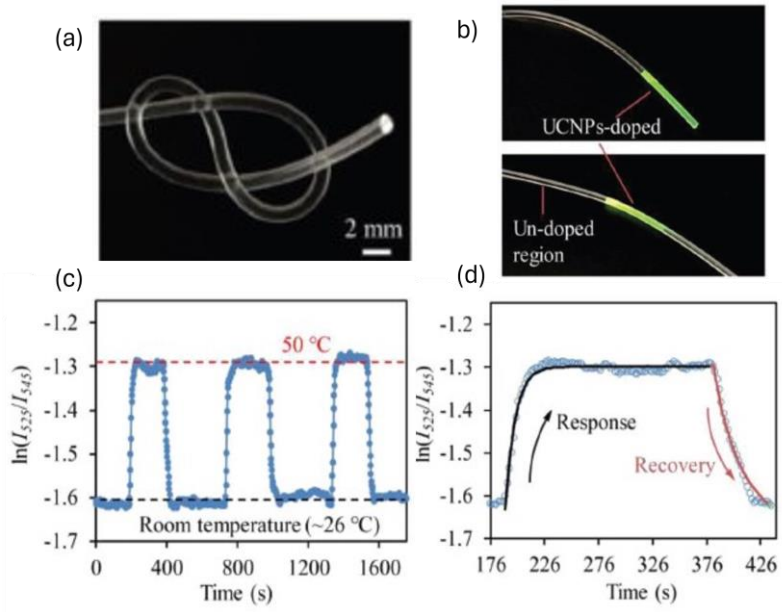

Figure 11. (**a**) Mechanical flexibility of stretchable polymer optical fiber sensors, (**b**) visible upconversion emissions at a temperature-sensitive upconversion-nanoparticle (UCNP)-loaded site in stretchable polymer optical fiber (PDMS) when illuminated with 980 nm laser, (**c**) cycling test of PDMS-UCNP-based temperature sensor, (**d**) response and recovery behavior of a PDMS-UCNP based temperature sensor. Reproduced with permission from [3].

3.6. Molecularly Imprinted Polymers (MIPs)

MIPs are a special class of synthetic materials that mimic the molecular recognition process of biological macromolecules, such as substrate-enzyme or antigen–antibody interactions. The working principle of MIPs is based on the creation of template-shaped cavities in a polymer matrix, which have a high predetermined affinity for their target molecule [12]. The molecular imprinting process involves several steps, including template selection, functional monomer selection, polymerization, template removal, and binding. MIPs have several advantages over natural receptors, such as low cost, robustness, unlimited shelf life, and animal-free technology [132]. MIPs have been used in various biomedical applications, including biosensors, electrochemical sensors, optical sensors, viral detection, and bacterial detection [132,133]. For instance, adenovirus-imprinted particles have been created to detect adenovirus with high specificity and sensitivity. The MIP-based SPR sensor demonstrated specific recognition of adenovirus in the concentration range of 0.01–20 pM, with a detection limit of 0.02 pM [134]. Another example presents the development of a highly selective and sensitive optical sensor for detecting isopropanol (IPA) vapor using molecularly imprinted polymers (MIPs). This sensor, designed for potential biomedical applications like non-invasive diabetes monitoring, is portable and efficient. It demonstrates high sensitivity, with maximum sensitivities of 0.37, 0.30, 0.62, and 0.63 nm/%IPA for exposure times of 30, 60, 90, and 120 min, respectively. The sensor's selectivity among similar volatile organic compounds (VOCs) further underscores its potential for practical use in detecting IPA as a biomarker in exhaled breath [135]. Another finding showcased usage of MIP-titanium oxide hybrid thin films on LPG using poly(acrylic acid) polymer for label-free creatinine detection (critical in the diagnosis of kidney diseases). The molecularly imprinted films exhibit a binding constant of 67/M, significantly enhancing sensitivity by ninefold compared to non-imprinted films. Refractive index changes upon creatinine binding changes coupling conditions of LPG, resulting in measurable wavelength shifts [136]. MIP-coated optical fiber–polymer waveguide–optical fiber (OFWF) structure was demonstrated for

attogram sensing via fluorescence detection, making it promising for ultrasensitive real-time biosensing [137]. OFs at ends are used for launching and collecting fluorescence light, whereas MIP coating of 1.5 µm on polymer waveguide (1,6-hexanediol diacrylate and 3,4-epoxycyclohexylmethyl-3,4-epoxycyclo-hexanecarboxylate) forms a sensing probe by acting as a functional monomer, which forms a polymer matrix with cavities matching the shape and size of target molecules. The sensor achieves an extremely low detection limit, approximately 6.5×10^{-17} g/mL (20–30 attograms), making it highly sensitive for detecting trace amounts of analytes. Figure 12(1) demonstrates MIP-based OFWF configuration, optical characteristics, and a MIP-coated waveguide sensor probe. A similar MIP-coated (thickness: 1.5–2 µm) OF—waveguide hybrid structure probe, with an extremely low limit of detection of 0.27 aM, was utilized for florescence sensing by utilizing high efficiency (98%) of light propagation from waveguide core to the MIP sensing layer, demonstrating its possible usage for detection of biomolecules and biological mechanisms in living systems [138]. Figure 12(2) depicts an MIP-based hybrid waveguide structure, fabrication, and optical characteristics, along with the extraction efficiency of the MIP layer. In both examples, the sensing mechanism is different from evanescent-based sensing since there is a large refractive index difference between the MIP sensing layer and the waveguide core, thus efficiently confining light in the MIP sensing layer, whose high porosity can help penetrate analyte molecules.

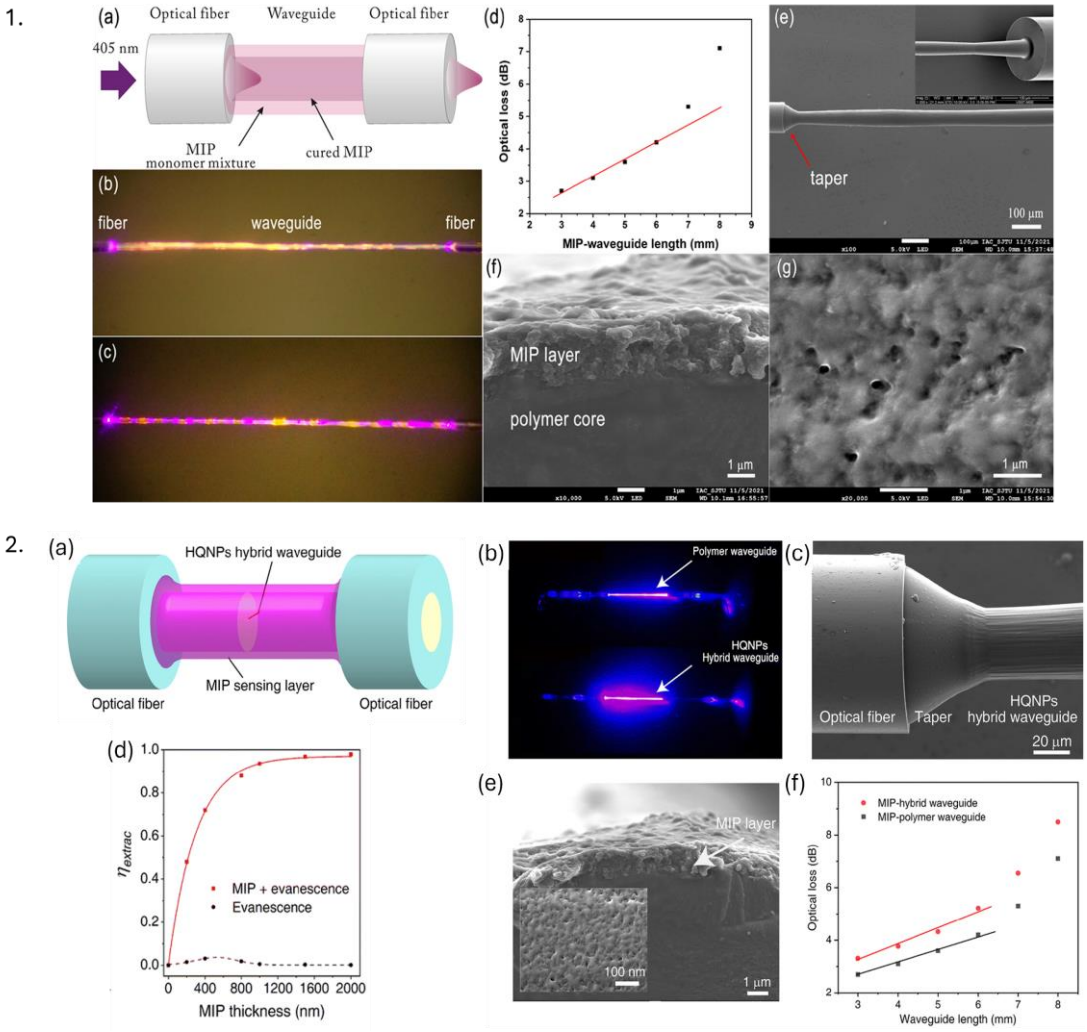

Figure 12. 1. (**a**) Schematic of an OF–waveguide–OF (OFWF) structure with the MIP coating process (**b**,**c**) microscopic images of a MIP-coated waveguide when irradiated with 405 nm. (**d**) Optical

loss of MIP coated OFWF structure, SEM images of (**e**) MIP-OFWF structure, (**f**) cross-section of a MIP-coated waveguide, and (**g**) MIP surface layer. Reproduced with permission from [137]. **2**. (**a**) Simulation of a MIP—hybrid probe, (**b**) Pure polymer waveguide loss in comparison with a hollow quartz nanoparticle (HQNP) hybrid optical sensor, (**c**) SEM image of joint of MIP-hybrid optical sensor, (**d**) simulation-based extraction efficiency (η_{extrac}) with respect to MIP layer thickness for evanescent wave only and its integration with light confined in the MIP layer, (**e**) SEM image of the cross-section of MIP coated waveguide sensing probe and (**f**) comparison of optical loss between MIP—hybrid OFWF and MIP—polymer OFWF. Reproduced with permission from [138].

In the realm of polymer-based optical sensors, MIPs have been incorporated to construct optical sensors that can detect specific molecules by monitoring changes in optical signals, such as variations in fluorescence, absorbance, or refractive index (as in the aforementioned examples), thereby offering a versatile platform for molecular detection. Despite the notable advantages of MIPs in biomedical sensing applications in terms of high selectivity, sensitivity, and robustness, the development of MIPs for biomedical applications faces several challenges, such as the need for optimization of the imprinting process, the potential for non-specific binding, and the need for validation in complex biological matrices.

4. Overview of Various Fabrication Techniques and Applications

Several fabrication techniques are utilized for POFs and PCOFs. Major manufacturing techniques include thermal drawing, batch and continuous extrusion, photochemical polymerization, chemical vapor deposition, and melt and dry spinning processes. These techniques are suitable for producing microstructured, step, and graded index POF. For PCOFs, techniques such as dip coating, spin coating, injection molding, layer-by-layer assembly, and plasma polymerization are commonly used to apply polymer coatings on standard silica optical fibers. The basics of fabrication and usage applications for a few of these techniques are described below.

4.1. Thermal Drawing

The thermal drawing technique involves creating a preform, a larger piece of polymer, clamping it at a holding fixture, and heating it at elevated temperatures (above glass transition temperature). This leads to a decrease in viscosity, which forces it to transition from a solid to a viscous state, thus drawing it down into a thinner fiber. This method allows for the fabrication of fibers with complex geometries and multiple layers, which can enhance the optical performance and functionality of the fibers. Thermal drawing is especially useful for producing fibers with specific optical properties tailored for biomedical applications, such as shape-memory fibers that can adapt to their environment and multifunctional fiber integration [31,122]. M.J. Antonini et al. used an iterative thermal drawing procedure to fabricate a versatile multifunctional optical fiber probe for a neural interface capable of recording spontaneous neural activity in mice for several weeks [139]. Chi Lu et al. fabricated a bifunctional polymer fiber probe consisting of PC as the core, cyclic olefin copolymer as the cladding, and carbon black-doped conductive polyethylene as the electrode for electrical recording and optical stimulation of neural activity in the spinal cord of mice having channelrhodopsin-2 as a light sensitive protein with an optical attenuation of ∼2.32 dB/cm [140], as shown in Figure 13(1). Yu et al., have showcased the potential use of thermally drawn PC and PMMA-based porous OF for localized drug delivery for cancer treatment [141], illustrated in Figure 13(2). Critical parameters such as the temperature of the oven, molecular weight distribution of polymer, and drawing speed influence the optical and mechanical characteristics of POFs. H. Banerjee et al. used thermal drawing as a scalable and alternative platform to manufacture step-index soft multi-material fibers (e.g., poly(styrene-b-(ethylene-co-butylene)-b-styrene) as the core and Geniomer as cladding) with a propagation loss of 0.5 dB/cm for potential applications as a stretchable waveguide for medical devices and implants [142,143]. The thermal drawing method is traditionally used to create step-index POFs with uniform diameters (typically

0.5–1.0 mm with drawing speeds of 0.2–0.5 m/s) for long-range production, though it can only be used with polymers that can be thermally processed without degradation, i.e., materials should have similar melting temperatures, glass transition temperatures, and thermal expansion coefficients for a smooth co-drawing process [144].

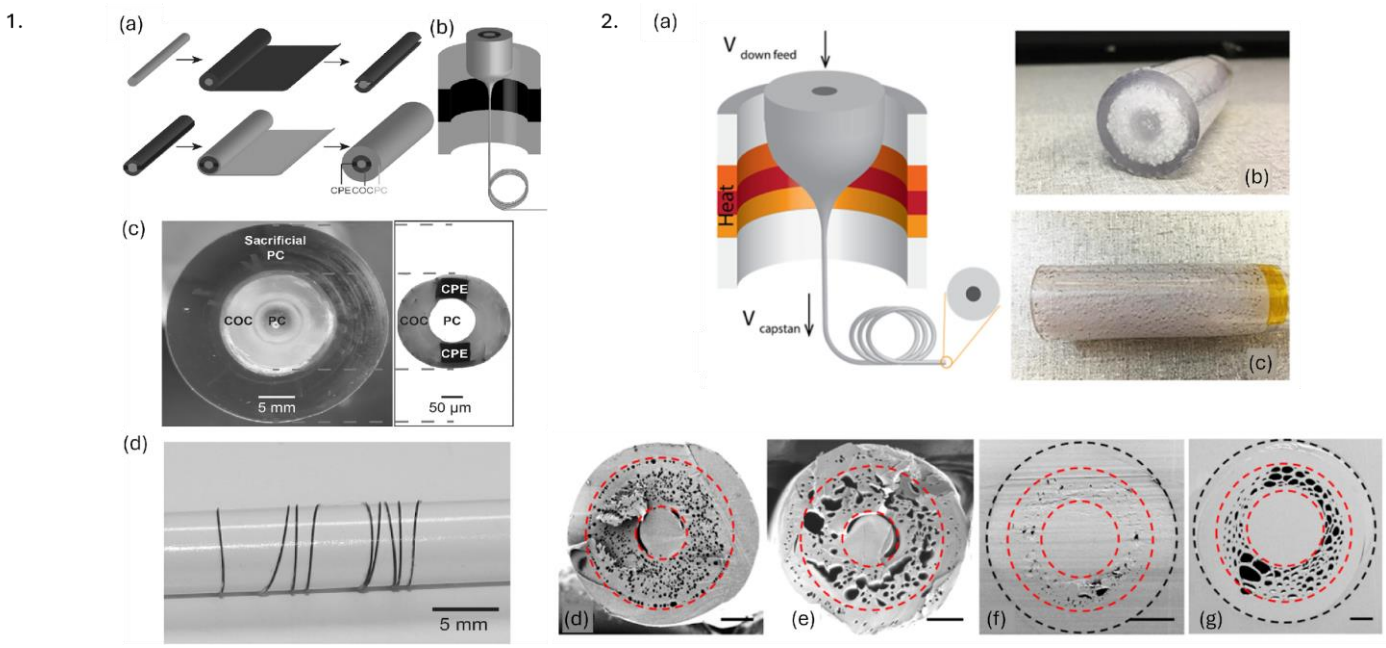

Figure 13. 1. Fabrication process of polymer neural fiber probe. (**a**) Preform fabrication, (**b**) thermal drawing of preform into fiber, (**c**) cross-section of preform consisting of PC core, cyclic olefin copolymer as cladding, and carbon black-doped conductive polyethylene as electrode. (**d**) Etched neural probe wrapped around pencil. Reproduced from [140]. **2**. (**a**) Thermal drawing of optical fibers from (**b**,**c**) PC preforms (**b**). (**d**–**f**) SEM images of cross sections of porous optical fibers; (**f**,**g**) represent this fiber embedded inside resin. Reprinted with permission from [141] © Optical Society of America.

4.2. Extrusion

The extrusion method involves modifying the viscosity of the polymer by temperature and forcing it through a die to create a continuous fiber. The shape of the die can be adjusted to produce fibers with various cross-sectional geometries, like circular, elliptical, and other complex shapes. This technique is typically used for high-throughput production and for creating microstructured optical fibers preforms. To produce inorganic optical fibers, Gallichi-Nottiani et al. fabricated microstructured OFs of 125 µm through extrusion of bioresorbable calcium–phosphate glass [145]. Extrusion-based 3D-printing techniques have been explored for manufacturing microstructured POF (Figure 14(1)) with propagation loss of 1.1 dB/cm at 1557 nm [146]. Figure 14(2) depicts a cross-sectional image of extruded microstructured fiber of 800 µm diameter and near-field transmitted light at 1550 nm. The batch extrusion technique is normally used to fabricate step-index polymer fibers. They are ideal for small-scale production in the laboratory and prototyping as they allow detailed control over fiber composition, which is particularly useful in tissue engineering scaffolds and personalized drug delivery. Continuous extrusion is efficient for large-scale production due to its exceptional purity and is suitable for wearable and implantable devices requiring continuous monitoring of physiological parameters. The co-extrusion process allows the possibility of multi-layered fibers with diverse functionalities suitable for multifunctional sensors.

1.

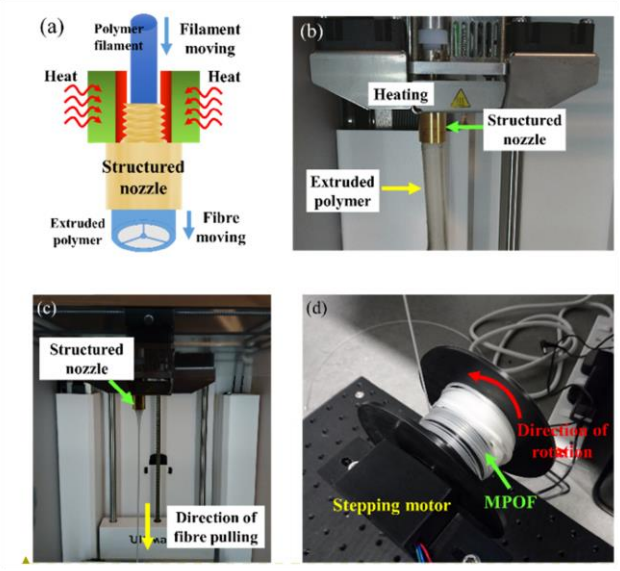

2.

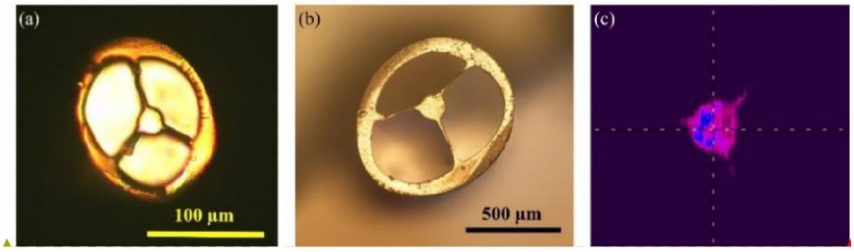

Figure 14. 1. (**a**) Representation and (**b**) experimental setup for microstructured polymer optical fiber extrusion; (**c**) fiber drawn from structured nozzle; (**d**) microstructured fiber wrapped around 3D printed spool connected to stepper motor. **2**. (**a**,**b**) Microscope images of fiber cross section at different diameters; (**c**) near field image of transmitted light at 1550 nm for full turn bending of 12.5 mm radius. Reprinted from [146], under CC 4.0, https://creativecommons.org/licenses/by/4.0/, (accessed on 7 September 2024).

Though this technique allows the production of fibers with consistent diameters and the possibility of incorporating additives and materials to enhance optical properties, precise control of processing parameters is required to ensure optical quality. Also, the high temperature required for the extrusion process can lead to thermal degradation of particular polymers, reducing the optical and mechanical properties of fibers.

4.3. Laser Writing

Laser writing methodologies are commonly used for fabricating various types of PFBGs. Major fabrication techniques include phase mask and femtosecond writing. Phase mask writing utilizes diffractive grating to modulate UV laser beams (typically, 248 nm, 266 nm, and 325 nm) into a periodic pattern (+1/−1 or 0/−1 orders), creating interference patterns to generate refractive index modulations producing gratings on POFs. This method is quite straightforward and does not require complex optical setups, thus making it suitable for mass production. The gratings produced are of high quality with well-defined reflection peaks. However, it is highly sensitive to alignment, especially between the phase masks and the OF. Also, the grating characteristics and, thus, Bragg wavelength are determined by phase mask design and period, thereby limiting customization and multiplexing options. The Talbot interferometer is coupled with this technique to overcome this issue, but at the expense of adding complexity to the setup. J. Bonefecacino et al. demonstrated PMMA-based FBG inscription in just 7 ms using a 325 nm He-Cd laser, the FBG inscription setup has been depicted in Figure 15a. They used this technique to monitor respiratory and heart rate with 30 times greater wavelength shifts than standard silica fibers [147] (Figure 15b–d).

Furthermore, X. Hu et al. demonstrated the fabrication of 3° tilted FBGs on PMMA fiber with a refractive index sensitivity of 13 nm/RIU [86].

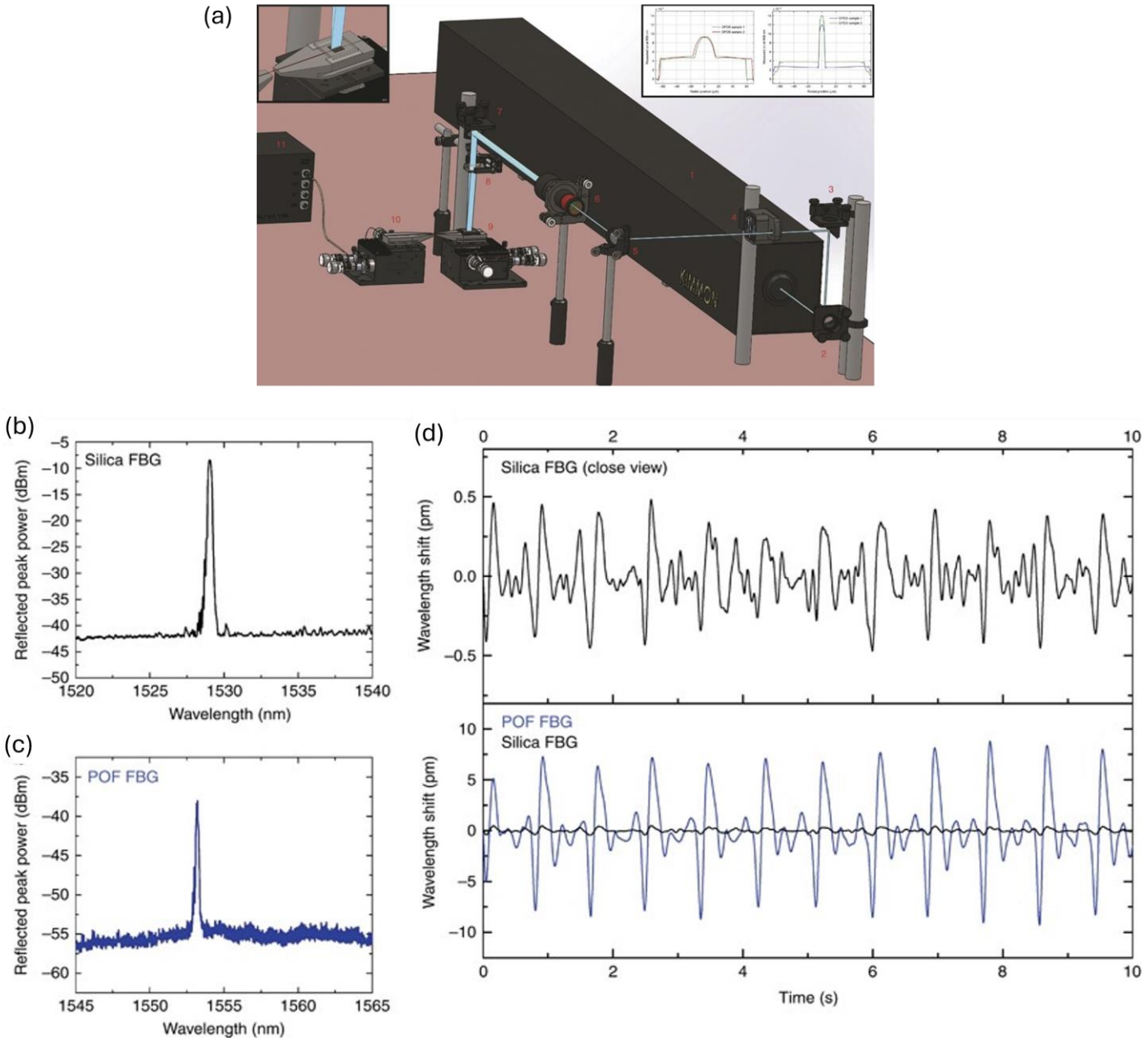

Figure 15. (**a**) Millisecond grating inscription inside a PMMA OF using 325 nm He-Cd laser. (**b**) Refection spectra of standard silica FBG. (**c**) Reflection spectra of 7 ms PFBG. (**d**) Filtered reflection wavelength shift of silica (in black) and polymer (in blue). Reprinted from [147], under CC 4.0, https://creativecommons.org/licenses/by/4.0/, (accessed on 7 September 2024).

Femtosecond laser writing uses ultra-short pulses and high peak power to induce non-linear absorption in polymers, resulting in localized refractive index changes, allowing direct writing of complex grating structures without significant thermal effects. Although this technique causes minimal thermal damage and has high spatial resolution, it requires sophisticated optical setups with expensive laser systems. Also, not all polymers show adequate photosensitivity for femtosecond laser writing. The point-by-point technique involves the sequential inscription of individual grating segments along the length of the fiber. It allows room for high precision and flexibility and, thereby, customization of grating

parameters. It also minimizes thermal effects due to minimal thermal diffusion, preserving the integrity and quality of gratings. However, the process is quite time-consuming, especially with high-density grating patterns, and requires sophisticated systems for high precision controls. On the other hand, the plane-by-plane technique provides simultaneous inscription of multiple grating planes across fiber cross-sections. This method is more efficient and faster, capable of inscribing entire grating planes in a single exposure; however, it provides limited room for customization.

J.N. Dash et al. fabricated a novel rectangular 2 mm long PFBG using a 520 nm fs laser using point-by-point technique, with a strain and temperature sensitivity of 1.29 pm/με and 15 pm/°C at 1511.3 nm [148]. In contrast, Leal Junior et al. manufactured 5 FBG arrays in CYTOP fiber using the fs plane-by-plane technique for multiparameter sensing in smart walkers for individuals undergoing physical rehabilitation to monitor and estimate gait cadence, human-robot interaction, and floor vibration conditions. The strain and temperature sensitivities were found to be 1.57 pm/με and 20.17 pm/°C, respectively [141].

4.4. Microfabrication

Microfabrication techniques such as hot embossing, photolithography, and nanoimprint lithography are more commonly used as fabrication techniques for polymer-based optical waveguides. In POFs, these methods are employed to create intricate microstructures on the optical fiber surface or at its tip. These techniques allow the integration of functional features such as surface modifications, microchannels, and gratings. Photolithography involves several steps involving the application of light-sensitive photoresist to the substrate, exposing it to UV radiation through a mask, and developing a pattern to create microstructures. Usually, this method is used to fabricate microfluidic devices, biosensors, and patterned substrates for cell culture. This technique has also been utilized to create microstructures and microchannels in polymer-based lab-on-chip devices for the detection of biomarkers in a small volume of biological fluids. For instance, PMMA-based step index polymer fiber was embedded inside PDMS photonic skin consisting of U-shaped grooves of 150 μm, fabricated using a soft lithography approach for potential wearable sensor application [149]. In an alternative study, a novel method using nanosphere lithography (NSL) to create nanopatterns on optical fiber tips involved the self-assembly of PS nanospheres (dimensions of 200–600 nm) into a hexagonal array on the water surface, which is then transferred onto the optical fiber tips for potential biosensing applications. The lithographic process allows for precise and reproducible patterning, enhancing the optical properties and sensitivity of the fibers [150].

Etching, both wet and dry, further refines these microstructures by selectively removing material, thereby improving light propagation and sensitivity in applications like biosensing and drug delivery systems. By way of illustration, chemical wet etching of PMMA/poly(vinylidene difluoride)—core/cladding POF was carried out using a dibromomethane solution to achieve compound parabolic concentrator at tip fiber for enhancing efficiency of fluorescence glucose sensor by a factor of 3.16 compared to sensors with plane-cut surfaces [151]. Figure 16 illustrates the etching mechanism, the formation of the parabolic tip, and average detected spectra of parabolic and plane-cut OF sensors. Additionally, techniques such as electron beam and soft lithography enable the creation of sub-micro and nanoscale features on flexible devices that can conform to irregularly shaped objects, enhancing their functionality in clinical settings. These techniques are typically used for developing planar and flexible sensors for microarray creation, utilized for high-throughput screening of biomolecules, protein interaction during drug development, and genetic markers for cancer. This method provides high precision and control over microstructures while enabling the development of complicated fiber designs at the expense of complex and expensive cleanroom processes.

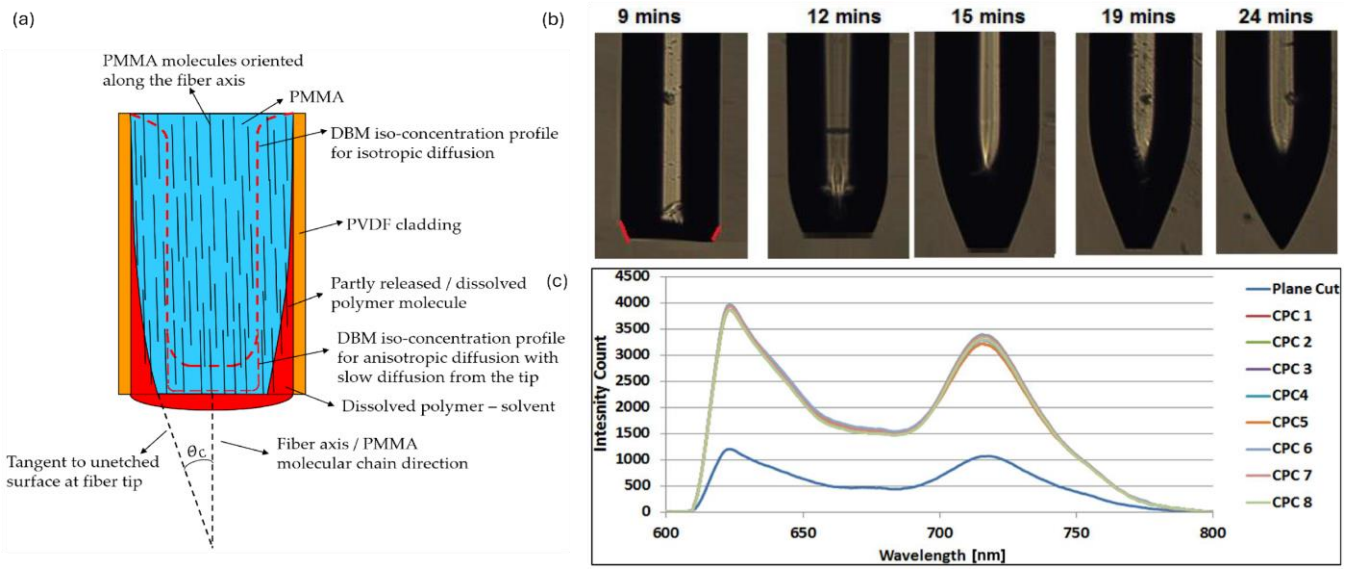

Figure 16. (**a**) Illustration of an etching mechanism. (**b**) Formation of compound parabolic concentrator at different etching times. (**c**) Spectrum of compound parabolic concentrator and plane-cut tip sensor. Reprinted from [151], under CC 4.0, https://creativecommons.org/licenses/by/4.0/, (accessed on 7 September 2024).

4.5. Dip Coating, Spin Coating, and Injection Molding

Dip coating is a widely used method that involves immersing silica OFs into a polymer solution, allowing the polymer to adhere to the fiber as it is withdrawn at a controlled speed. This allows a thin film of polymer to form and solidify on the fiber surface. The procedure is simple, cost-effective, and suitable for fabricating uniform coatings over long fiber lengths. Thickness control can be challenging due to the requirement of precise regulation over the withdrawal speed, which depends on the viscosity of the solution, and the possibility of wasting polymer solution. This approach has been used to create biocompatible uniform coatings of PDMS on OFs functionalized with fluorophore for monitoring UV emissions from biochemical species and for sensing temperature [49].

Spin coating is another predominant technique where a small amount of polymer solution is placed on fiber and spun at high speeds, thereby spreading polymer uniformly via centrifugal force. This method allows precise control over coating thickness, uniformity, and reproducibility. However, it is limited to small lengths of fiber and planar coatings. It also requires precise control of spin speed and solution viscosity. A.K. Manocchi et al. demonstrated the use of biodegradable planar optical waveguides fabricated via spin coating, potentially for implantable biomedical devices [152]. J.S. Kee also fabricated a single-mode PDMS waveguide for a possible lab-on-chip application [153].

Injection molding involves the placement of an OF inside a 3D-printed mold. A liquid polymer is then injected into the mold, encapsulating the fiber and allowing the creation of uniform and precise coatings. These 3D-printed molds can be created with precise thickness, tolerance, and length of polymer coatings. The fiber, along with the mold, is then cured using thermal or UV light, depending on the polymer used. Though 3D printing allows customization and precision, there are limitations on the choice of 3D printed materials that are compatible with the polymer and optical fibers in terms of adhesion and printing resolution. It can be used to coat only a particular section of a fiber. The PDMS/THV (terpolymer of tetrafluoroethylene, hexafluoropropylene, and vinylidene fluoride)-core/clad POF core was fabricated using the molding in tube strategy, whereas cladding was manufactured using dip coating for real-time continuous monitoring of human body movements [154] (Figure 17). This technique along with spin coating was also utilized to fabricate MZI-evanescent wave sensing-based planar integrated optical waveguides were fabricated for enabling highly sensitive label-free detection of

biomolecules which also allows for cost-effective production of these disposable sensor chips [155]. In another study, biocompatible silicone coating of 3mm diameter and 54cm length on a standard FBG was fabricated using injection molding for in-vivo pressure detection [109]. A synthesis of key parameters of the aforementioned fabrication techniques is shown in Table 4.

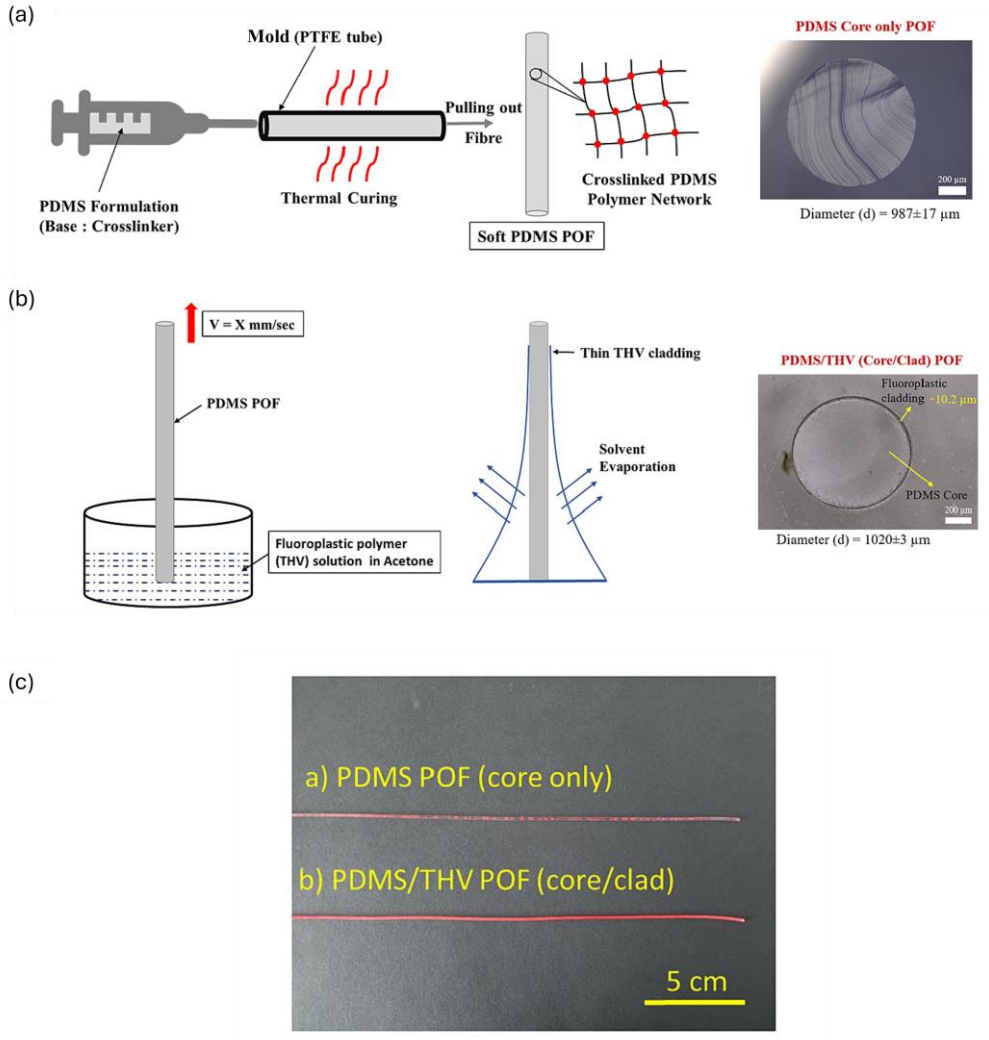

Figure 17. (**a**) Injection molding strategy for fabricating PDMS cores in PTFE tube molds. (**b**) Dip coating of PDMS core inside the THV (terpolymer of tetrafluoroethylene, hexafluoropropylene, and vinylidene fluoride) polymer solution to process the THV clad of 10 µm. (**c**) PDMS and PDMS/THV coated with Lumogen red dye. Reprinted from [154], under CC 4.0, https://creativecommons.org/licenses/by/4.0/, (accessed on 7 September 2024).

Table 4. Comparison of fabrication techniques for polymer optical fibers and polymer coatings on standard optical fibers and their relevant usage in biomedical applications.

Fabrication Technique	Advantages	Disadvantages	Applications
Thermal drawing	• Enables fabrication of multifunctional fibers with tailored optical properties • Suitable for producing long, uniform-diameter fibers	• Limited to thermally stable polymers • Requires precise control over drawing parameters	• Neural interfaces for recording activity [139,140] • Porous fibers for localized drug delivery [141] • Stretchable waveguides for medical devices [142,143]
Extrusion	• High-throughput production • Ability to create microstructured and multi-layered fibers for multifunctional sensors	• Precise control of processing parameters (temperature, pressure, etc.) is critical • High temperatures may degrade sensitive polymers	• Wearable and implantable devices [145,146] • Tissue engineering scaffolds • Personalized drug delivery systems

Table 4. *Cont.*

Fabrication Technique	Advantages	Disadvantages	Applications
Laser writing(phase mask and femtosecond laser)	• High precision and customization of grating parameters • Minimal thermal damage (with femtosecond lasers)	• Expensive and sophisticated equipment required • Time-consuming for complex patterns • Limited polymer photosensitivity	• Refractive index-based biochemical sensing [86] • Sensors for respiratory and heart rate monitoring [147] • Multiparameter sensing in rehabilitation devices [141,148]
Microfabrication(photolithography, nanoimprint lithography)	• High precision in creating intricate microstructures • Enables complex fiber designs and surface modifications	• Requires expensive cleanroom facilities • Time-consuming fabrication processes	• Lab-on-chip devices for biomarker detection [149] • Nanopatterned fibers for biosensing [150] • Microarrays for drug development and genetic analysis
Dip coating	• Simple and cost-effective method • Suitable for uniform coatings over long fibers	• Thickness control can be challenging • Potential wastage of polymer solution	• Temperature and UV emission sensors [49] • Biocompatible coatings for biomedical implants • Fluorescence-based sensors
Spin coating	• Precise control over coating thickness and uniformity • High reproducibility	• Limited to small fiber lengths and planar surfaces • Requires precise control of spin parameters	• Implantable biomedical devices [152] • Planar optical waveguides for lab-on-chip applications [152,153] • Single-mode waveguides
Injection molding	• •Allows for uniform and precise coatings • Customizable mold designs with precise dimensions • Effective for coating only specific fiber sections	• Limited compatible materials among mold, polymer, and fiber • Not scalable for coating long lengths of OFs	• Sensors for real-time continuous monitoring [154] • Mach–Zehnder Interferometer (MZI) optical waveguides [155] • Integrated optical devices with precise geometries

4.6. Polymer-Coated Sensors for Biomedical Catheters and Guidewires

Standard FBGs have limitations on strain and temperature sensitivity due to silica glass's strain-optic, thermo-optic, and thermal expansion coefficients as explained in Section 2.3. These limitations restrict their effectiveness in biomedical applications requiring very high sensitivities, especially in minimally invasive applications. As detailed in Section 2.4, polymer coating amplifies these parameters by acting as a transducer.

Zhang et al. developed microstructured OFs for in vivo pressure detection. The sensor design involved hyperelastic packaging of ultrashort, weak FBGs to enhance later strain and pressure sensitivity for measuring pressure waves inside the esophagus. Two ultrashort FBGs represented microstructure with low finesse Fabry–Perot. The device had an outer diameter of 3 mm with a spatial resolution of 10 mm with a pressure sensitivity of 2.2 nm/MPa. Theoretically, 243 sensing microstructures could be multiplexed in single fiber using this methodology [109]. J.W. Arkwright et al. reported FBG sensing based on silicone flexible diaphragms adhering to the rigid metallic substrate for in vivo monitoring of peristalsis in the esophagus. The catheter's outer diameter was around 3 mm with each FBG length of 3 mm and FWHM of 0.6 nm. They used 32 wavelength division multiplexed FBGs with a spatial resolution of 10 mm to measure pressure in the range of 0–150 mmHg [156]. D.H. Wang et al. used two coiled FBGs (with coinciding positions) enclosed inside a silicone diaphragm and glued to cylindrical metal castings for monitoring peristalsis in the gastrointestinal tract. The detection mechanism is based on the pressure-induced differential Bragg wavelength. This configuration has inherent temperature compensation since the sensor would cause common mode variation not relating to pressure differential wavelength shift. The spatial resolution of the device is 10 mm, and the silicone diaphragm diameter is 1 mm [157]. J.W. Arkwright et al. also reported a high sensor count manometry catheter for recording peristalsis in the human colon and diagnosing colonic motility disorders. Two fibers, each with a 32 FBG sensor array, are woven into the biocompatible elastomeric sleeves. The catheter diameter was observed to be 2.2 mm with a pressure sensitivity of 1 pm/mmHg with a dynamic range of 1200 mmHg [158]. S. Voigt et al. developed two catheter designs for high-resolution manometry applications. The first design utilized a dual-layer polymer coating with thermoplastic elastomers of Shore

hardness 30 A and 80 A, with a total diameter of 3 mm on an 80 µm FBG to effectively convert radial strain into axial strain. The second design employed a single 3 mm PDMS coating on a 125 µm FBG. The pressure sensitivities of these designs were 0.7 µε/mbar and 0.5 µε/mbar, respectively. Additionally, the catheter design incorporated 32 multiplexed sensors with a spatial resolution of 10 mm [159]. In a similar investigation, M. Becker reported a silicone polymeric-coated FBG-based array sensor also used for high-resolution manometry applications. The outer diameter of the device was 3 mm, with a fiber diameter of 80 um, a spatial resolution of 1 cm, and a pressure resolution of 1 mbar. Thirty-two FBG sensors were multiplexed with 1 cm spacing, and coatings of soft (shore 30 A), hard (shore 80 A), and hybrid (30 A and 80 A) thermoplastic polymers with pressure sensitivities of 1.2 µε/mbar, 0.7 µε/mbar, and 0.45 µε/mbar were utilized [160]. Ulacia et al. developed novel 355.6 µm OF-based pressure guidewire physiological pressure index measurements. The design involved Fabry–Perot interferometry with a silicone diaphragm at the tip of multimode OF(Figure 18). The silicone diaphragm's corrugated configuration drastically reduces the impact of moisture and temperature. The sensor diameter is around 200 µm for a possible dynamic range from −300 mmHg to 350 mmHg, with a precision of 1 mmHg and resolution of 0.2 mmHg [161]. C.R. Dennisson et al. increased the pressure sensitivity (7.8 fm/mmHg) by 20 times than that of standard FBG by reducing optical fiber diameter down to 25 µm along with polymeric packaging using silicone and epoxy, resulting in a 200 µm device diameter for biomedical pressure sensing measurements such as cerebrospinal fluid and blood pressure measurements [162]. The device resolution obtained was 2.7 mmHg with a pressure range of 0–1875 mmHg. A different study by Dennisson et al. used a packaged FBG-based pressure sensor consisting of silicone and a hyperdermic tube for ex vivo intervertebral disc pressure sensor measurements in porcine discs. The sensor diameter and pressure sensitivity were determined to be 400 µm and −21.5 pm/µε, respectively [111]. In a different investigation, M. Friedemann et al. presented an integrated fiber tip Fabry–Perot interferometer (FTFPI) and an FBG as a pressure sensor catheter for potentially monitoring real-time blood pressure and diagnosing conditions such as lumbar spinal stenosis. The sensor components are encapsulated within a 2 mm diameter silicone mantle, ensuring biocompatibility and durability for in vivo applications. The FTFPI provides high-resolution pressure sensing while the FBG compensates for temperature variations, enhancing measurement accuracy. The device's pressure and temperature sensitivities were measured as—3 pm/mbar and 101 pm/K for the FTFPI, and 0.03 pm/mbar and 15.6 pm/K for the FBG. The resolution of the FTFPI was determined to be 2 mbar [163]. Table 5 summarizes key parameters essential for pressure sensing using guidewires or catheters enhanced with polymer-assisted optical sensing technologies.

Table 5. Summary of key parameters and applications of polymer-assisted sensing for physiological monitoring.

Polymer Coating/Supporting Material	Sensor Type	Key Parameters	Application(s)	Reference No.
Hyperelastic packaging using silicone rubber	FBG	OD: 3 mm SR: 10 mm PS: 0.29 pm/mmHg	High-resolution manometry	[109]
Silicone	FBG	OD: 400 µm PS: −2.87 fm/mmHg Coating length: 50 mm Coating thickness: 0.1 mm	Intervertebral disc pressure sensing	[111]
Silicone rubber as diaphragms	FBG	OD: 3 mm SR: 10 mm PR: 3.1 mmHg Range: 0–150 mmHg	In vivo monitoring of peristalsis in the esophagus, monitoring peristaltic wave in gastrointestinal tract	[156]
Silicone diaphragm enclosing coiled FBGs	FBG	OD: 1 mm SR: 10 mm	Peristalsis in the gastrointestinal tract	[157]
Biocompatible—elastomeric sleeve	FBG	OD: 2.2 mm PS: 1 pm/mmHg	Diagnosing colonic motility disorders	[158]

Table 5. *Cont.*

Polymer Coating/Supporting Material	Sensor Type	Key Parameters	Application(s)	Reference No.
PDMS and silicone	FBG	OD: 5 mm SR:10 mm PS: 0.67 με/mmHg	High-resolution manometry	[159]
Two-layer silicone (shore 30 A and 80 A)	FBG	OD: 3 mm SR:1 cm	High-resolution manometry	[160]
Silicone diaphragm in Fabry–Perot-based sensing	Fabry–Perot	OD: 355.6 μm PR: 0.2 mmHg Range: −300 to 350 mmHg	Coronary physiology	[161]
Silicone- and epoxy- aided	FBG	OD: 200 μm PS: −7.8 fm/mmHg PR: 2.7 mmHg Range: 0–1875 mmHg Coating length: 1.4 mm Coating thickness: 140 μm	Biomedical pressure sensing	[162]
Silicone	Fabry–Perot and FBG	Coating length: 2 mm PS: 3.99 pm/mmHg PR: 1.5 mmHg	Pressure sensor catheter	[163]

OD: outer device diameter, SR: Spatial resolution, PR: pressure resolution, PS: pressure sensitivity

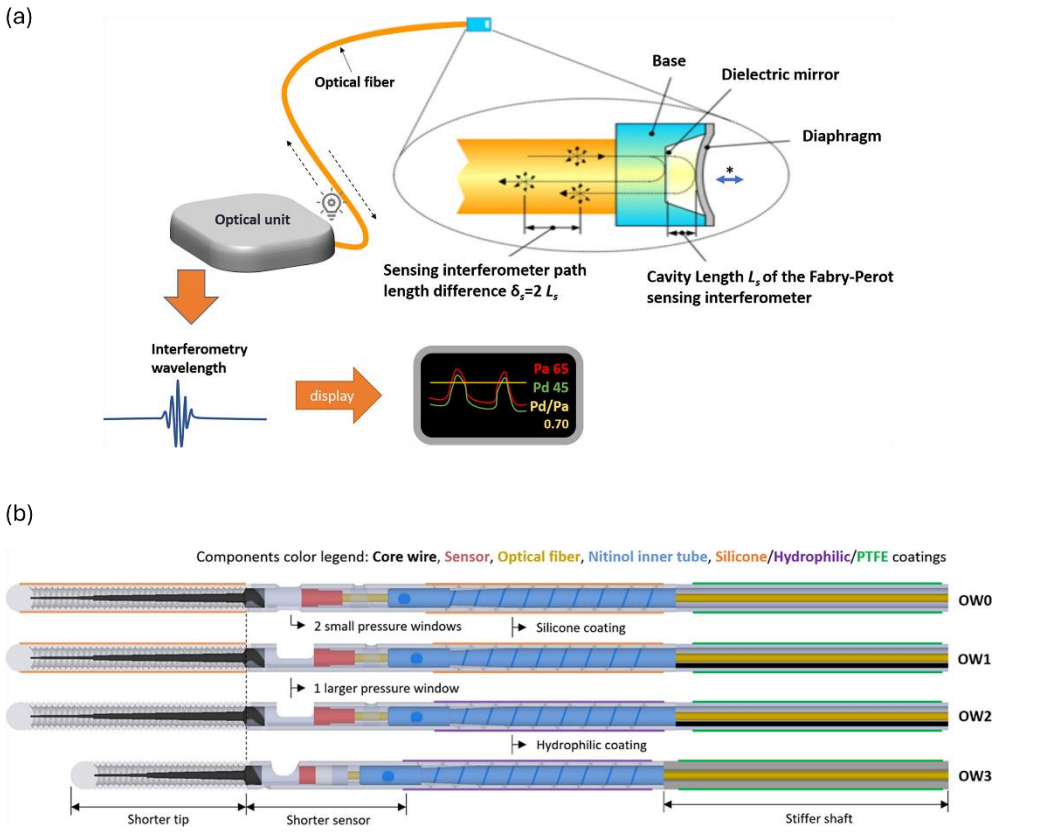

Figure 18. (**a**) Polymer diaphragm-assisted Fabry–Perot-based pressure transducer for coronary physiological pressure assessment. Light signal is sent to pressure transducer via optical fiber, which gets perturbed in response to diaphragm's deflection changes due to arterial pressure affecting path length of transmitted light. The optical unit identifies interferometry wavelength and maps it to the applied pressure for visualization. (**b**) Design evolution of the OptoWire (OW) pressure guidewire. Reproduced with permission from [161].

5. Conclusions and Perspectives

This review provides an overview of polymer-based optical sensors in biomedical applications. It elucidates their fundamental characteristics, various categories, and sub-

categories of optical sensor configuration, polymer materials, fabrication techniques, and application in biomedical sensing disciplines. Special emphasis is placed on PFBGs and polymer-coated FBGs, widely employed in this sector for both ex vivo and in vivo diagnostic and monitoring procedures as single and multi-point sensors. The selection of materials consists of biocompatible, biodegradable, hydrophilic, stimuli-responsive, conductive, elastomeric, and molecularly imprinted polymers, and their typical usage in certain biomedical applications was also discussed. A glimpse of common fabrication techniques such as thermal drawing, extrusion, microfabrication, laser writing, injection molding, and dip and spin coating was also presented, highlighting their benefits and drawbacks in biomedical applications. Specific attention is given to polymer-coated FBGs used extensively in biomedical catheters and guidewires. The discussion also focuses on the specific benefits and potential constraints of each fabrication method, providing a thorough grasp of their utility in improving the performance and functionality of biomedical devices.

POW sensors are advantageous for applications requiring high sensitivity and integration into miniaturized devices. At the same time, these sensors often require fabrication processes involving precise lithography and etching, which can increase production costs and limit scalability. While polymers offer mechanical flexibility, the rigidity of substrates used in waveguide sensors may limit their application in wearable or implantable devices that require conformity to dynamic biological environments.

Luminescent sensors offer high selectivity and sensitivity, which can detect minute changes in analyte concentrations. Nevertheless, these sensors can be susceptible to photobleaching and environmental degradation, potentially affecting long-term stability and accuracy. Some polymers can mitigate these issues by protecting luminescent materials, but careful design is necessary to ensure durability and consistent performance.

SPR sensors offer ultra-high sensitivity for label-free, real-time detection of biomolecular interactions and are particularly suitable for applications such as early-stage cancer biomarker detection, pathogen identification, and drug-target interaction studies. Their main disadvantage is that they often require complex fabrication processes and can be more expensive due to the use of noble metals like gold and silver.

POF sensors combine mechanical flexibility with enhanced strain and temperature sensitivities, making them well-suited for wearable health monitoring devices; nonetheless, they are hindered by higher optical losses, repeatability of measurements, and cross-sensitivities due to environmental factors like humidity and temperature.

PCOF sensors combine the robustness of silica fibers with the functional advantages of polymers. Polymer coatings can enhance sensitivity and selectivity by acting as transducers responding to specific analytes or environmental changes. PCOFs have shown significant potential in minimally invasive biomedical applications, such as pressure guidewires and catheters. The main challenges with these sensors include potential coating degradation in biological environments and the fair adhesion of polymers to the silica fiber surface, which plays a crucial role in the sensor's performance. Despite these challenges, the potential of PCOF sensors is promising, offering scope for further developments in sensitivity, resolution, and specificity in biomedical sensing applications. Selecting the appropriate sensor technology requires a tradeoff between sensor parameters and the specific requirements of the biomedical application.

The future of POS in bio-photonics depends on advances in material research, fabrication processes, and sensor integration. Improving polymer biocompatibility and biodegradability is crucial for long-term implant safety and effectiveness. Innovations in 3D printing and nano-imprinting will result in more complex and compact sensor designs with higher performance. The focus will be on multiparameter sensing capabilities, which allow for the simultaneous monitoring of numerous physiological markers to improve diagnostic accuracy. Furthermore, improving the sensitivity and specificity of these sensors, particularly for identifying low-abundance biomarkers, is a major difficulty. Distributed sensing methods, notably those that use FBGs, Rayleigh, and Brillouin scattering, can be further explored to provide high-resolution spatial monitoring, which is critical for tissue engineering and

oncology applications. Addressing these problems through interdisciplinary research and innovation is essential to leveraging the full potential of POS in healthcare. Furthermore, overcoming sensor metrics problems, such as strain and temperature cross-sensitivity, linearity, resolution, limit of detection, and response time, as evidenced by advances in polymer coatings and novel sensor configurations, may expand the use of these sensors in minimally invasive and highly sensitive biomedical sensing contexts.

Funding: This research was funded by the European Union's Horizon 2020 research and innovation programme under the Marie Sklodowska-Curie grant agreement No. 860185, as part of PHAST-ITN project.

Data Availability Statement: Not applicable.

Conflicts of Interest: The authors declare no conflicts of interest.

Abbreviations

CP	Conductive polymer
CYTOP	Fluorinated polymer
DOFS	Distributed optical fiber sensors
EMI	Electromagnetic interference
FBG	Fiber Bragg gratings
FTFPI	Fiber tip Fabry—Perot interferometer
LPG	Long-Period gratings
MIP	Molecularly imprinted polymers
NIR	Near-Infrared
OF	Optical fiber
OHD	Hydroxyvitamin-D
PC	Polycarbonate
PCOF	Polymer-coated optical fibers
PDMS	Polydimethylsiloxane
PEG	Polyethylene glycol
PEGDA	Poly(ethylene glycol) diacrylate
PFBGs	Polymer fiber Bragg gratings
PGA	Polyglycolic acid
PLA	Polylactic acid
PMMA	Poly(methyl methacrylate)
POF	Polymer optical fibers
POS	Polymer-based optical sensor
POW	Polymer-based optical waveguides
PPy	Polypyrrole
PS	Polystyrene
PVA	Poly(vinyl alcohol)
SPP	Surface plasmon polaritons
SPR	Surface plasmon resonance
UCNP	Upconversion nanoparticles

References

1. Ngiejungbwen, L.A.; Hamdaoui, H.; Chen, M.-Y. Polymer optical fiber and fiber Bragg grating sensors for biomedical engineering Applications: A comprehensive review. *Opt. Laser Technol.* **2024**, *170*, 110187. [CrossRef]
2. Nazempour, R.; Zhang, Q.; Fu, R.; Sheng, X. Biocompatible and Implantable Optical Fibers and Waveguides for Biomedicine. *Materials* **2018**, *11*, 1283. [CrossRef] [PubMed]
3. Guo, J.; Zhou, B.; Yang, C.; Dai, Q.; Kong, L. Stretchable and Temperature—Sensitive Polymer Optical Fibers for Wearable Health Monitoring. *Adv. Funct. Mater.* **2019**, *29*, 1902898. [CrossRef]
4. Global Biomedical Sensor Market Size by Type (Wireless, Wired), By Sensor Type (Pressure, Temperature), By Industry (Healthcare, Pharmaceutical), By Geographic Scope and Forecast. Available online: https://www.verifiedmarketresearch.com/product/biomedical-sensor-market/ (accessed on 31 July 2024).
5. Medical Fiber Optics Market Size, Share & Growth & Trends Analysis Report By Fiber Type (Multimode, Plastic), By Product Type (Fiber Optics Cables), By Application, By Region, And Segment Forecasts, 2023–2030. Available online: https://www.grandviewresearch.com/industry-analysis/medical-fiber-optics-market (accessed on 27 August 2024).

6. Lopes, R.N.; Pinto, P.H.S.; Vargas, J.D.L.; Dante, A.; Macrae, A.; Allil, R.C.B.; Werneck, M.M. Development of an Immunocapture-Based Polymeric Optical Fiber Sensor for Bacterial Detection in Water. *Polymers* **2024**, *16*, 861. [CrossRef] [PubMed]
7. Mizuno, Y.; Theodosiou, A.; Kalli, K.; Liehr, S.; Lee, H.; Nakamura, K. Distributed polymer optical fiber sensors: A review and outlook. *Photon. Res.* **2021**, *9*, 1719–1733. [CrossRef]
8. Hema, M.; Suman, J.V.; Kumar, B.K.; Haile, A. Design and Development of Polymer-Based Optical Fiber Sensor for GAIT Analysis. *Int. J. Polym. Sci.* **2023**, *2023*, 2541384. [CrossRef]
9. Yang, W.; Ma, Y.; Sun, H.; Huang, C.; Shen, X. Molecularly imprinted polymers based optical fiber sensors: A review. *TrAC Trends Anal. Chem.* **2022**, *152*, 116608. [CrossRef]
10. Ahmed, I.; Ali, M.; Elsherif, M.; Butt, H. UV polymerization fabrication method for polymer composite based optical fiber sensors. *Sci. Rep.* **2023**, *13*, 10823. [CrossRef]
11. Guo, Y.; Dai, K. Soft and Stretchable Polymeric Optical Waveguide-Based Sensors for Wearable and Biomedical Applications. *Sensors* **2019**, *19*, 3771. [CrossRef]
12. Alam, M.W.; Islam Bhat, S.; Al Qahtani, H.S.; Aamir, M.; Amin, M.N.; Farhan, M.; Aldabal, S.; Khan, M.S.; Jeelani, I.; Nawaz, A.; et al. Recent Progress, Challenges, and Trends in Polymer-Based Sensors: A Review. *Polymers* **2022**, *14*, 2164. [CrossRef]
13. Leal-Junior, A.G.; Diaz, C.A.R.; Avellar, L.M.; Pontes, M.J.; Marques, C.; Frizera, A. Polymer Optical Fiber Sensors in Healthcare Applications: A Comprehensive Review. *Sensors* **2019**, *19*, 3156. [CrossRef] [PubMed]
14. Grattan, K.T.V.; Sun, T. Fiber optic sensor technology: An overview. *Sens. Actuators A Phys.* **2000**, *82*, 40–61. [CrossRef]
15. Mishra, V.; Singh, N.; Tiwari, U.; Kapur, P. Fiber grating sensors in medicine: Current and emerging applications. *Sens. Actuators A Phys.* **2011**, *167*, 279–290. [CrossRef]
16. Correia, R.; James, S.; Lee, S.-W.; Morgan, S.P.; Korposh, S. Biomedical application of optical fibre sensors. *J. Opt.* **2018**, *20*, 073003. [CrossRef]
17. Shakir, A.D. Optical Fiber Sensors for Biomedical Applications of Optical Fibers, Fiber Sensors, Impact of Light and Healthcare Industry Trends. *J. Curr. Med. Res. Opinion* **2023**, *6*, 1849–1855. Available online: https://cmro.in/index.php/jcmro/article/view/668 (accessed on 6 August 2024).
18. Marques, C.A.F.; Webb, D.J.; Andre, P. Polymer optical fiber sensors in human life safety. *Opt. Fiber Technol.* **2017**, *36*, 144–154. [CrossRef]
19. Khonina, S.N.; Voronkov, G.S.; Grakhova, E.P.; Kazanskiy, N.L.; Kutluyarov, R.V.; Butt, M.A. Polymer Waveguide-Based Optical Sensors—Interest in Bio, Gas, Temperature, and Mechanical Sensing Applications. *Coatings* **2023**, *13*, 549. [CrossRef]
20. Zhang, W.; Webb, D.J.; Peng, G.-D. Investigation into Time Response of Polymer Fiber Bragg Grating Based Humidity Sensors. *J. Light. Technol.* **2012**, *30*, 1090–1096. [CrossRef]
21. Yang, D.X.; Yu, J.; Tao, X.; Tam, H. Structural and mechanical properties of polymeric optical fiber. *Mater. Sci. Eng. A* **2004**, *364*, 256–259. [CrossRef]
22. Oliveira, R.; Sequeira, F.; Bilro, L.; Nogueira, R. Polymer Optical Fiber Sensors and Devices. In *Handbook of Optical Fibers*; Peng, G.-D., Ed.; Springer: Singapore, 2018; pp. 1–41. ISBN 978-981-10-1477-2.
23. Leal-Junior, A.; Theodosiou, A.; Frizera-Neto, A.; Pontes, M.J.; Shafir, E.; Palchik, O.; Tal, N.; Zilberman, S.; Berkovic, G.; Antunes, P.; et al. Characterization of a new polymer optical fiber with enhanced sensing capabilities using a Bragg grating. *Opt. Lett.* **2018**, *43*, 4799–4802. [CrossRef]
24. Silva-López, M.; Fender, A.; MacPherson, W.N.; Barton, J.S.; Jones, J.D.C.; Zhao, D.; Dobb, H.; Webb, D.J.; Zhang, L.; Bennion, I. Strain and temperature sensitivity of a single-mode polymer optical fiber. *Opt. Lett.* **2005**, *30*, 3129–3131. [CrossRef] [PubMed]
25. Bhowmik, K.; Peng, G.-D. Polymer Optical Fibers. In *Handbook of Optical Fibers*; Peng, G.-D., Ed.; Springer: Singapore, 2019; pp. 1–51. ISBN 978-981-10-1477-2.
26. Luo, Y.; Yan, B.; Zhang, Q.; Peng, G.-D.; Wen, J.; Zhang, J. Fabrication of Polymer Optical Fibre (POF) Gratings. *Sensors* **2017**, *17*, 511. [CrossRef] [PubMed]
27. Wei, H.; Chen, M.; Krishnaswamy, S. Three-dimensional-printed Fabry–Perot interferometer on an optical fiber tip for a gas pressure sensor. *Appl. Opt.* **2020**, *59*, 2173–2178. [CrossRef] [PubMed]
28. Choi, C.-G.; Kim, J.-T.; Jeong, M.-Y. Fabrication of optical waveguides in thermosetting polymers using hot embossing. In Proceedings of the Integrated Photonics Research, Optica Publishing Group, Washington, DC, USA, 15–20 June 2003; p. ITuH6.
29. Yetisen, A.K.; Jiang, N.; Fallahi, A.; Montelongo, Y.; Ruiz-Esparza, G.U.; Tamayol, A.; Zhang, Y.S.; Mahmood, I.; Yang, S.-A.; Kim, K.S.; et al. Glucose-Sensitive Hydrogel Optical Fibers Functionalized with Phenylboronic Acid. *Adv. Mater.* **2017**, *29*, 1606380. [CrossRef]
30. Guo, J.; Zhou, M.; Yang, C. Fluorescent hydrogel waveguide for on-site detection of heavy metal ions. *PubMed* **2017**, *7*, 7902. Available online: https://pubmed.ncbi.nlm.nih.gov/28801653/ (accessed on 6 August 2024). [CrossRef] [PubMed]
31. Wang, Y.; Huang, Y.; Bai, H.; Wang, G.; Hu, X.; Kumar, S.; Min, R. Biocompatible and Biodegradable Polymer Optical Fiber for Biomedical Application: A Review. *Biosensors* **2021**, *11*, 472. [CrossRef]
32. Zhang, M.; Zhang, W.; Wang, F.; Zhao, D.; Qu, C.; Wang, X.; Yi, Y.; Cassan, E.; Zhang, D. High-gain polymer optical waveguide amplifiers based on core-shell $NaYF_4/NaLuF_4$: Yb^{3+}, Er^{3+} NPs-PMMA covalent-linking nanocomposites. *Sci. Rep.* **2016**, *6*, 36729. [CrossRef]

33. Singer, J.A.; Stramm, T.; Fasel, J.; Schween, O.; Gelaeschus, A.; Bahr, A.; Kuhl, M. Flexible Polymer Optical Waveguides for Integrated Optogenetic Brain Implants. In Proceedings of the 2023 IEEE 36th International Conference on Micro Electro Mechanical Systems (MEMS), Munich, Germany, 15–19 January 2023; pp. 370–373.
34. Ioannides, N.; Chunga, E.B.; Bachmatiuk, A.; Gonzalez-Martinez, I.G.; Trzebicka, B.; Adebimpe, D.B.; Kalymnios, D.; Rümmeli, M.H. Approaches to mitigate polymer-core loss in plastic optical fibers: A review. *Mater. Res. Express* **2014**, *1*, 032002. [CrossRef]
35. Kazanskiy, N.L.; Butt, M.A.; Svetlana, N. Khonina. Recent Advances in Wearable Optical Sensor Automation Powered by Battery versus Skin-like Battery-Free Devices for Personal Healthcare—A Review. *Nanomaterials* **2022**, *12*, 334. [CrossRef]
36. Choi, M.; Humar, M.; Kim, S.; Yun, S.-H. Step-Index Optical Fiber Made of Biocompatible Hydrogels. *Adv. Mater.* **2015**, *27*, 4081–4086. [CrossRef]
37. Choi, M.; Choi, J.W.; Kim, S.; Nizamoglu, S.; Hahn, S.K.; Yun, S.H. Light-guiding hydrogels for cell-based sensing and optogenetic synthesis in vivo. *Nat. Photon* **2013**, *7*, 987–994. [CrossRef] [PubMed]
38. Prajzler, V.; Min, K.; Kim, S.; Nekvindova, P. The Investigation of the Waveguiding Properties of Silk Fibroin from the Visible to Near-Infrared Spectrum. *Materials* **2018**, *11*, 112. [CrossRef] [PubMed]
39. Shan, D.; Zhang, C.; Kalaba, S.; Mehta, N.; Kim, G.B.; Liu, Z.; Yang, J. Flexible biodegradable citrate-based polymeric step-index optical fiber. *Biomaterials* **2017**, *143*, 142–148. [CrossRef] [PubMed]
40. Kozma, P.; Kehl, F.; Ehrentreich-Förster, E.; Stamm, C.; Bier, F.F. Integrated planar optical waveguide interferometer biosensors: A comparative review. *Biosens. Bioelectron.* **2014**, *58*, 287–307. [CrossRef] [PubMed]
41. Irawan, R.; Cheng, Y.H.; Ng, W.M.; Aung, M.M.; Lao, I.K.; Thaveeprungsriporn, V. Polymer waveguide sensor for early diagnostic and wellness monitoring. *Biosens. Bioelectron.* **2011**, *26*, 3666–3669. [CrossRef]
42. Pediredla, A.; Scopelliti, M.G.; Narasimhan, S.; Chamanzar, M.; Gkioulekas, I. Optimized virtual optical waveguides enhance light throughput in scattering media. *Nat. Commun.* **2023**, *14*, 5681. [CrossRef]
43. Yang, J.-M.; Yang, N.-Z.; Chen, C.-H.; Huang, C.-S. Gradient Waveguide Thickness Guided-Mode Resonance Biosensor. *Sensors* **2021**, *21*, 376. [CrossRef]
44. Prasanna Kumaar, S.; Sivasubramanian, A. Analysis of BCB and SU 8 photonic waveguide in MZI architecture for point-of-care devices. *Sens. Int.* **2023**, *4*, 100207. [CrossRef]
45. Olyaee, S.; Mohebzadeh-Bahabady, A. Two-curve-shaped biosensor using photonic crystal nano-ring resonators. *J. Nanostructures* **2014**, *4*, 303–308. [CrossRef]
46. Wolfbeis, O.S. Luminescent sensing and imaging of oxygen: Fierce competition to the Clark electrode. *Bioessays* **2015**, *37*, 921–928. [CrossRef]
47. Hong, S.; Pawel, G.T.; Pei, R.; Lu, Y. Recent progress in developing fluorescent probes for imaging cell metabolites. *Biomed. Mater.* **2021**, *16*, 044108. [CrossRef] [PubMed]
48. Yang, Y.; Zhang, Y.; Xie, S.; Tang, Y.; Zeng, Z.; Tang, B.Z. Hydrogel-derived luminescent scaffolds for biomedical applications. *Mater. Chem. Front.* **2021**, *5*, 3524–3548. [CrossRef]
49. Carrillo-Betancourt, R.A.; López-Camero, A.D.; Hernández-Cordero, J. Luminescent Polymer Composites for Optical Fiber Sensors. *Polymers* **2023**, *15*, 505. [CrossRef] [PubMed]
50. De Acha, N.; Elosua, C.; Matias, I.; Arregui, F.J. Luminescence-Based Optical Sensors Fabricated by Means of the Layer-by-Layer Nano-Assembly Technique. *Sensors* **2017**, *17*, 2826. [CrossRef]
51. Pirzada, M.; Altintas, Z. Recent Progress in Optical Sensors for Biomedical Diagnostics. *Micromachines* **2020**, *11*, 356. [CrossRef]
52. Burmistrova, N.A.; Kolontaeva, O.A.; Duerkop, A. New Nanomaterials and Luminescent Optical Sensors for Detection of Hydrogen Peroxide. *Chemosensors* **2015**, *3*, 253–273. [CrossRef]
53. Li, Y.; Luo, S.; Gui, Y.; Wang, X.; Tian, Z.; Yu, H. Difunctional Hydrogel Optical Fiber Fluorescence Sensor for Continuous and Simultaneous Monitoring of Glucose and pH. *Biosensors* **2023**, *13*, 287. [CrossRef]
54. Guo, J.; Zhou, B.; Yang, C.; Dai, Q.; Kong, L. Stretchable and upconversion-luminescent polymeric optical sensor for wearable multifunctional sensing. *Opt. Lett.* **2019**, *44*, 5747–5750. [CrossRef]
55. Janith, G.I.; Herath, H.S.; Hendeniya, N.; Attygalle, D.; Amarasinghe, D.A.S.; Logeeshan, V.; Wickramasinghe, P.M.T.B.; Wijayasinghe, Y.S. Advances in surface plasmon resonance biosensors for medical diagnostics: An overview of recent developments and techniques. *J. Pharm. Biomed. Anal. Open* **2023**, *2*, 100019. [CrossRef]
56. Douzi, B. Protein-Protein Interactions: Surface Plasmon Resonance. In *Bacterial Protein Secretion Systems*; Humana Press: New York, NY, USA, 2017; Volume 1615, pp. 257–275. [CrossRef]
57. Michaelis, S.; Wegener, J.; Robelek, R. Label-free monitoring of cell-based assays: Combining impedance analysis with SPR for multiparametric cell profiling. *Biosens. Bioelectron.* **2013**, *49*, 63–70. [CrossRef]
58. Hammond, J.L.; Bhalla, N.; Rafiee, S.D.; Estrela, P. Localized Surface Plasmon Resonance as a Biosensing Platform for Developing Countries. *Biosensors* **2014**, *4*, 172–188. [CrossRef] [PubMed]
59. Shui, X.; Gu, Q.; Jiang, X.; Si, G. Surface Plasmon Resonance Sensor Based on Polymer Liquid-Core Fiber for Refractive Index Detection. *Photonics* **2020**, *7*, 123. [CrossRef]
60. Wang, Y.; Rao, X.; Wu, X.; Chen, G.Y.; Liao, C.; Smietana, M.J.; Wang, Y. Highly-Sensitive Polymer Optical Fiber SPR Sensor for Fast Immunoassay. *Photonic Sens.* **2024**, *14*, 240413. [CrossRef]
61. Cennamo, N.; Pasquardini, L.; Arcadio, F.; Vanzetti, L.E.; Bossi, A.M.; Zeni, L. D-shaped plastic optical fibre aptasensor for fast thrombin detection in nanomolar range. *Sci. Rep.* **2019**, *9*, 18740. [CrossRef] [PubMed]

62. Walter, J.-G.; Alwis, L.S.M.; Roth, B.; Bremer, K. All-Optical Planar Polymer Waveguide-Based Biosensor Chip Designed for Smartphone-Assisted Detection of Vitamin D. *Sensors* **2020**, *20*, 6771. [CrossRef] [PubMed]
63. Zhang, W.; Webb, D.J. Humidity responsivity of poly(methyl methacrylate)-based optical fiber Bragg grating sensors. *Opt. Lett.* **2014**, *39*, 3026–3029. [CrossRef]
64. Leal-Junior, A.G.; Marques, C.; Frizera, A.; Pontes, M.J. Dynamic Mechanical Analysis on a PolyMethyl Methacrylate (PMMA) Polymer Optical Fiber. *IEEE Sens. J.* **2018**, *18*, 2353–2361. Available online: https://ieeexplore.ieee.org/document/8267228 (accessed on 1 June 2024). [CrossRef]
65. Leal-Junior, A.; Frizera, A.; Marques, C.; Pontes, M.J. Polymer-optical-fiber-based sensor system for simultaneous measurement of angle and temperature. *Appl. Opt.* **2018**, *57*, 1717–1723. [CrossRef]
66. Leal-Junior, A.; Frizera, A.; Lee, H.; Mizuno, Y.; Nakamura, K.; Paixão, T.; Leitão, C.; Domingues, M.F.; Alberto, N.; Antunes, P.; et al. Strain, temperature, moisture, and transverse force sensing using fused polymer optical fibers. *Opt. Express* **2018**, *26*, 12939–12947. Available online: https://opg.optica.org/oe/fulltext.cfm?uri=oe-26-10-12939&id=386169 (accessed on 1 July 2024). [CrossRef]
67. Antunes, P.F.C.; Varum, H.; André, P.S. Intensity-Encoded Polymer Optical Fiber Accelerometer. *IEEE Sens. J.* **2013**, *13*, 1716–1720. [CrossRef]
68. Bilro, L.; Alberto, N.; Pinto, J.L.; Nogueira, R. Optical Sensors Based on Plastic Fibers. *Sensors* **2012**, *12*, 12184–12207. [CrossRef] [PubMed]
69. Leitão, C.; Antunes, P.; Pinto, J.L.; Bastos, J.M.; André, P. Carotid distension waves acquired with a fiber sensor as an alternative to tonometry for central arterial systolic pressure assessment in young subjects. *Measurement* **2017**, *95*, 45–49. [CrossRef]
70. Leal-Junior, A.G.; Frizera, A.; Vargas-Valencia, L.; dos Santos, W.M.; Bó, A.P.L.; Siqueira, A.A.G.; Pontes, M.J. Polymer Optical Fiber Sensors in Wearable Devices: Toward Novel Instrumentation Approaches for Gait Assistance Devices. *IEEE Sens. J.* **2018**, *18*, 7085–7092. [CrossRef]
71. Tu, X.; Chen, S.-L.; Song, C.; Huang, T.; Guo, L.J. Ultrahigh Q Polymer Microring Resonators for Biosensing Applications. *IEEE Photonics J.* **2019**, *11*, 4200110. [CrossRef]
72. Ramirez, J.C.; Lechuga, L.M.; Gabrielli, L.H.; Hernandez-Figueroa, H.E. Study of a low-cost trimodal polymer waveguide for interferometric optical biosensors. *Opt. Express* **2015**, *23*, 11985–11994. [CrossRef]
73. Bruck, R.; Melnik, E.; Muellner, P.; Hainberger, R.; Lämmerhofer, M. Integrated polymer-based Mach-Zehnder interferometer label-free streptavidin biosensor compatible with injection molding. *Biosens. Bioelectron.* **2011**, *26*, 3832–3837. [CrossRef]
74. Roriz, P.; Frazão, O.; Lobo-Ribeiro, A.B.; Santos, J.L.; Simoes, J.A. Review of fiber-optic pressure sensors for biomedical and biomechanical applications. *J. Biomed. Opt.* **2013**, *18*, 050903. [CrossRef]
75. Wang, L.; Fang, N.; Wang, L.; Fang, N. Applications of Fiber-Optic Interferometry Technology in Sensor Fields. In *Optical Interferometry*; IntechOpen: Rijeka, Croatia, 2017; ISBN 978-953-51-2956-1.
76. Min, R.; Ortega, B.; Marques, C. Latest Achievements in Polymer Optical Fiber Gratings: Fabrication and Applications. *Photonics* **2019**, *6*, 36. [CrossRef]
77. Liu, H.Y.; Liu, H.B.; Peng, G.D. Tensile strain characterization of polymer optical fibre Bragg gratings. *Opt. Commun.* **2005**, *251*, 37–43. [CrossRef]
78. Alwin, T. High sensitivity strain sensor based on Polymer Fiber Bragg Grating. In Proceedings of the 2023 IEEE 8th International Conference for Convergence in Technology (I2CT), Lonavla, India, 7–9 April 2023; pp. 1–4.
79. Pospori, A.; Ioannou, A.; Kalli, K. Temperature and Humidity Sensitivity of Polymer Optical Fibre Sensors Tuned by Pre-Strain. *Sensors* **2022**, *22*, 7233. [CrossRef]
80. Gouveia, C.A.J.; Baptista, J.M.; Jorge, P.A.S.; Gouveia, C.A.J.; Baptista, J.M.; Jorge, P.A.S. Refractometric Optical Fiber Platforms for Label Free Sensing. In *Current Developments in Optical Fiber Technology*; IntechOpen: Rijeka, Croatia, 2013; ISBN 978-953-51-1148-1.
81. Luo, B.-B.; Zhou, X.; Zhao, M.; Zhong, N.; Wang, S. Recent developments in microstructured fiber Bragg grating refractive index sensors. *Spie Rev.* **2010**, *1*, 018002. [CrossRef]
82. Rajan, G.; Bhowmik, K.; Xi, J.; Peng, G.-D. Etched Polymer Fibre Bragg Gratings and Their Biomedical Sensing Applications. *Sensors* **2017**, *17*, 2336. [CrossRef]
83. Bhowmik, K.; Ambikairajah, E.; Peng, G.-D.; Luo, Y.; Rajan, G. High-sensitivity polymer fibre Bragg grating sensor for biomedical applications. In Proceedings of the 2016 IEEE Sensors Applications Symposium (SAS), Catania, Italy, 20–22 April 2016; pp. 1–5.
84. Pilla, P.; Manzillo, P.F.; Malachovska, V.; Buosciolo, A.; Campopiano, S.; Cutolo, A.; Ambrosio, L.; Giordano, M.; Cusano, A. Long period grating working in transition mode as promising technological platform for label-free biosensing. *Opt. Express* **2009**, *17*, 20039–20050. [CrossRef]
85. Chiavaioli, F.; Biswas, P.; Trono, C.; Bandyopadhyay, S.; Giannetti, A.; Tombelli, S.; Basumallick, N.; Dasgupta, K.; Baldini, F. Towards sensitive label-free immunosensing by means of turn-around point long period fiber gratings. *Biosens. Bioelectron.* **2014**, *60*, 305–310. [CrossRef]
86. Hu, X.; Pun, C.-F.J.; Tam, H.-Y.; Mégret, P.; Caucheteur, C. Tilted Bragg gratings in step-index polymer optical fiber. *Opt. Lett.* **2014**, *39*, 6835–6838. [CrossRef]
87. Korganbayev, S.; Min, R.; Jelbuldina, M.; Hu, X.; Caucheteur, C.; Bang, O.; Ortega, B.; Marques, C.; Tosi, D. Thermal Profile Detection Through High-Sensitivity Fiber Optic Chirped Bragg Grating on Microstructured PMMA Fiber. *J. Light. Technol.* **2018**, *36*, 4723–4729. [CrossRef]

88. Marques, C.A.F.; Antunes, P.; Mergo, P.; Webb, D.J.; André, P. Chirped Bragg Gratings in PMMA Step-Index Polymer Optical Fiber. *IEEE Photonics Technol. Lett.* **2017**, *29*, 500–503. [CrossRef]
89. Deepa, S.; Das, B. Interrogation techniques for π-phase-shifted fiber Bragg grating sensor: A review. *Sens. Actuators A Phys.* **2020**, *315*, 112215. [CrossRef]
90. Ortega, B.; Min, R.; Sáez-Rodríguez, D.; Mi, Y.; Nielsen, K.; Bang, O. Bandpass transmission filters based on phase shifted fiber Bragg gratings in microstructured polymer optical fibers. In *Micro-structured and Specialty Optical Fibres V, Proceedings of the SPIE, Prague, Czech Republic, 16 May 2017*; SPIE: Bellingham, WA, USA, 2017; Volume 10232, pp. 23–33.
91. Pereira, L.M.; Pospori, A.; Antunes, P.; Domingues, M.F.; Marques, S.; Bang, O.; Webb, D.J.; Marques, C.A.F. Phase-Shifted Bragg Grating Inscription in PMMA Microstructured POF Using 248-nm UV Radiation. *J. Light. Technol.* **2017**, *35*, 5176–5184. [CrossRef]
92. Lo Presti, D.; Massaroni, C.; Jorge Leitão, C.S.; De Fátima Domingues, M.; Sypabekova, M.; Barrera, D.; Floris, I.; Massari, L.; Oddo, C.M.; Sales, S.; et al. Fiber Bragg Gratings for Medical Applications and Future Challenges: A Review. *IEEE Access* **2020**, *8*, 156863–156888. [CrossRef]
93. Katrenova, Z.; Alisherov, S.; Abdol, T.; Molardi, C. Status and future development of distributed optical fiber sensors for biomedical applications. *Sens. Bio-Sens. Res.* **2024**, *43*, 100616. [CrossRef]
94. Witt, J.; Narbonneau, F.; Schukar, M.; Krebber, K.; De Jonckheere, J.; Jeanne, M.; Kinet, D.; Paquet, B.; Depre, A.; D'Angelo, L.T.; et al. Medical Textiles with Embedded Fiber Optic Sensors for Monitoring of Respiratory Movement. *IEEE Sens. J.* **2012**, *12*, 246–254. [CrossRef]
95. Kanellos, G.T.; Papaioannou, G.; Tsiokos, D.; Mitrogiannis, C.; Nianios, G.; Pleros, N. Two dimensional polymer-embedded quasi-distributed FBG pressure sensor for biomedical applications. *Opt. Express* **2010**, *18*, 179–186. [CrossRef] [PubMed]
96. Leal-Junior, A.G.; Díaz, C.R.; Marques, C.; Pontes, M.J.; Frizera, A. Multiplexing technique for quasi-distributed sensors arrays in polymer optical fiber intensity variation-based sensors. *Opt. Laser Technol.* **2019**, *111*, 81–88. [CrossRef]
97. Katrenova, Z.; Alisherov, S.; Abdol, T.; Yergibay, M.; Kappassov, Z.; Tosi, D.; Molardi, C. Investigation of High-Resolution Distributed Fiber Sensing System Embedded in Flexible Silicone Carpet for 2D Pressure Mapping. *Sensors* **2022**, *22*, 8800. [CrossRef]
98. Mohanty, L.; Tjin, S.C. Pressure mapping at orthopaedic joint interfaces with fiber Bragg gratings. *Appl. Phys. Lett.* **2006**, *88*, 083901. [CrossRef]
99. Mizuno, Y.; Nakamura, K. Brillouin Scattering in Polymer Optical Fibers: Fundamental Properties and Potential Use in Sensors. *Polymers* **2011**, *3*, 886–898. [CrossRef]
100. Sapozhnikov, D.A.; Baiminov, B.A.; Vygodskii, Y.S. Highly Heat-Resistant Polymeric Coatings of Optical Fibers. *Polym. Sci. Ser. C* **2020**, *62*, 165–171. [CrossRef]
101. Li, C.; Yang, W.; Wang, M.; Yu, X.; Fan, J.; Xiong, Y.; Yang, Y.; Li, L. A Review of Coating Materials Used to Improve the Performance of Optical Fiber Sensors. *Sensors* **2020**, *20*, 4215. [CrossRef]
102. Bandyopadhyay, S.; Biswas, P.; Chiavaioli, F.; Dey, T.K.; Basumallick, N.; Trono, C.; Giannetti, A.; Tombelli, S.; Baldini, F.; Bandyopadhyay, S. Long-period fiber grating: A specific design for biosensing applications. *Appl. Opt.* **2017**, *56*, 9846–9853. Available online: https://opg.optica.org/ao/fulltext.cfm?uri=ao-56-35-9846&id=379371 (accessed on 6 August 2024). [CrossRef]
103. Rivero, P.J.; Goicoechea, J.; Arregui, F.J. Optical Fiber Sensors Based on Polymeric Sensitive Coatings. *Polymers* **2018**, *10*, 280. [CrossRef] [PubMed]
104. Hernández-Romano, I.; Monzón-Hernández, D.; Moreno-Hernández, C.; Moreno-Hernandez, D.; Villatoro, J. Highly Sensitive Temperature Sensor Based on a Polymer-Coated Microfiber Interferometer. *IEEE Photonics Technol. Lett.* **2015**, *27*, 2591–2594. [CrossRef]
105. Liu, Z.; Xiao, H.; Liao, M.; Han, X.; Chen, W.; Zhao, T.; Jia, H.; Yang, J.; Tian, Y. PDMS-Assisted Microfiber M-Z Interferometer with a Knot Resonator for Temperature Sensing. *IEEE Photonics Technol. Lett.* **2019**, *31*, 337–340. [CrossRef]
106. Rivero, P.J.; Urrutia, A.; Goicoechea, J.; Matias, I.R.; Arregui, F.J. A Lossy Mode Resonance optical sensor using silver nanoparticles-loaded films for monitoring human breathing. *Sens. Actuators B Chem.* **2013**, *187*, 40–44. [CrossRef]
107. Zhou, B.; Fan, K.; Li, T.; Luan, G.; Kong, L. A biocompatible hydrogel-coated fiber-optic probe for monitoring pH dynamics in mammalian brains in vivo. *Sens. Actuators B Chem.* **2023**, *380*, 133334. [CrossRef]
108. Dey, T.K.; Trono, C.; Biswas, P.; Giannetti, A.; Basumallick, N.; Baldini, F.; Bandyopadhyay, S.; Tombelli, S. Biosensing by Polymer-Coated Etched Long-Period Fiber Gratings Working near Mode Transition and Turn-around Point. *Biosensors* **2023**, *13*, 731. [CrossRef]
109. Zhang, W.; Ni, X.; Wang, J.; Ai, F.; Luo, Y.; Yan, Z.; Liu, D.; Sun, Q. Microstructured Optical Fiber Based Distributed Sensor for In Vivo Pressure Detection. *J. Light. Technol.* **2019**, *37*, 1865–1872. [CrossRef]
110. Xu, M.G.; Reekie, L.; Chow, Y.T.; Dakin, J.P. Optical in-fibre grating high pressure sensor. *Electronics Letters* **1993**, *29*, 398–399. [CrossRef]
111. Dennison, C.R.; Wild, P.M.; Wilson, D.R.; Cripton, P.A. A minimally invasive in-fiber Bragg grating sensor for intervertebral disc pressure measurements. *Meas. Sci. Technol.* **2008**, *19*, 085201. [CrossRef]
112. Nagar, M.A.; Lai, M.; Janner, D. Modified optical fiber sensors for intravital monitoring. In Proceedings of the Translational Biophotonics: Diagnostics and Therapeutics III, Munich, Germany, 25–29 June 2023; Optica Publishing Group: Washington, DC, USA, 2023; p. 126272U.

113. Shan, D.; Gerhard, E.; Zhang, C.; Tierney, J.W.; Xie, D.; Liu, Z.; Yang, J. Polymeric biomaterials for biophotonic applications. *Bioact. Mater.* **2018**, *3*, 434–445. [CrossRef]
114. Qiao, X.; Qian, Z.; Li, J.; Sun, H.; Han, Y.; Xia, X.; Zhou, J.; Wang, C.; Wang, Y.; Wang, C. Synthetic Engineering of Spider Silk Fiber as Implantable Optical Waveguides for Low-Loss Light Guiding. *ACS Appl. Mater. Interfaces* **2017**, *9*, 14665–14676. [CrossRef] [PubMed]
115. Nizamoglu, S.; Gather, M.C.; Humar, M.; Choi, M.; Kim, S.; Kim, K.S.; Hahn, S.K.; Scarcelli, G.; Randolph, M.; Redmond, R.W.; et al. Bioabsorbable polymer optical waveguides for deep-tissue photomedicine. *Nat. Commun.* **2016**, *7*, 10374. [CrossRef] [PubMed]
116. Savić Gajić, I.M.; Savić, I.M.; Svirčev, Z. Preparation and Characterization of Alginate Hydrogels with High Water-Retaining Capacity. *Polymers* **2023**, *15*, 2592. [CrossRef] [PubMed]
117. Shrivastav, A.M.; Gunawardena, D.S.; Liu, Z.; Tam, H.-Y. Microstructured optical fiber based Fabry–Pérot interferometer as a humidity sensor utilizing chitosan polymeric matrix for breath monitoring. *Sci. Rep.* **2020**, *10*, 6002. [CrossRef]
118. Hoffman, A.S. Stimuli-responsive polymers: Biomedical applications and challenges for clinical translation. *Adv. Drug. Deliv. Rev.* **2013**, *65*, 10–16. [CrossRef]
119. Shu, T.; Hu, L.; Shen, Q.; Jiang, L.; Zhang, Q.; Serpe, M.J. Stimuli-responsive polymer-based systems for diagnostic applications. *J. Mater. Chem. B* **2020**, *8*, 7042–7061. [CrossRef]
120. Bustamante-Torres, M.; Romero-Fierro, D.; Arcentales-Vera, B.; Palomino, K.; Magaña, H.; Bucio, E. Hydrogels Classification According to the Physical or Chemical Interactions and as Stimuli-Sensitive Materials. *Gels* **2021**, *7*, 182. [CrossRef]
121. Upadhyay, K.; Thomas, S.; Tamrakar, R.K.; Kalarikkal, N. Chapter 11—Functionalized photo-responsive polymeric system. In *Advanced Functional Polymers for Biomedical Applications*; Mozafari, M., Singh Chauhan, N.P., Eds.; Elsevier: Amsterdam, The Netherlands, 2019; pp. 211–233. ISBN 978-0-12-816349-8.
122. Strutynski, C.; Evrard, M.; Désévédavy, F.; Gadret, G.; Jules, J.-C.; Brachais, C.-H.; Kibler, B.; Smektala, F. 4D Optical fibers based on shape-memory polymers. *Nat. Commun.* **2023**, *14*, 6561. [CrossRef]
123. Zhu, Y.; Zhang, J.; Song, J.; Yang, J.; Du, Z.; Zhao, W.; Guo, H.; Wen, C.; Li, Q.; Sui, X.; et al. A Multifunctional Pro-Healing Zwitterionic Hydrogel for Simultaneous Optical Monitoring of pH and Glucose in Diabetic Wound Treatment. *Adv. Funct. Mater.* **2020**, *30*, 1905493. [CrossRef]
124. Kaur, G.; Adhikari, R.; Cass, P.; Bown, M.; Gunatillake, P. Electrically conductive polymers and composites for biomedical applications. *RSC Adv.* **2015**, *5*, 37553–37567. [CrossRef]
125. Ravichandran, R.; Sundarrajan, S.; Venugopal, J.R.; Mukherjee, S.; Ramakrishna, S. Applications of conducting polymers and their issues in biomedical engineering. *J. R. Soc. Interface* **2010**, *7*, S559–S579. [CrossRef] [PubMed]
126. Nezakati, T.; Seifalian, A.; Tan, A.; Seifalian, A.M. Conductive Polymers: Opportunities and Challenges in Biomedical Applications. *Chem. Rev.* **2018**, *118*, 6766–6843. [CrossRef] [PubMed]
127. Shahnia, S.; Rehmen, J.; Lancaster, D.G.; Monro, T.M.; Ebendorff-Heidepriem, H.; Evans, D.; Afshar, V.S. Towards new fiber optic sensors based on the vapor deposited conducting polymer PEDOT:Tos. *Opt. Mater. Express* **2019**, *9*, 4517–4531. Available online: https://opg.optica.org/ome/fulltext.cfm?uri=ome-9-12-4517&id=422859 (accessed on 6 August 2024). [CrossRef]
128. Cherpak, V.; Kremer, I.; Shandra, Z.; Hladun, M.; Lopatynskyy, A.; Lopatynska, O. Fiber-optic sensors based on conductive polymers. In Proceedings of the 2008 International Conference on "Modern Problems of Radio Engineering, Telecommunications and Computer Science" (TCSET), Lviv, Ukraine, 19–23 February 2008; pp. 489–490.
129. Canales, A.; Jia, X.; Froriep, U.P.; Koppes, R.A.; Tringides, C.M.; Selvidge, J.; Lu, C.; Hou, C.; Wei, L.; Fink, Y.; et al. Multifunctional fibers for simultaneous optical, electrical and chemical interrogation of neural circuits in vivo. *Nat. Biotechnol.* **2015**, *33*, 277–284. [CrossRef]
130. Park, S.; Guo, Y.; Jia, X.; Choe, H.K.; Grena, B.; Kang, J.; Park, J.; Lu, C.; Canales, A.; Chen, R.; et al. One-step optogenetics with multifunctional flexible polymer fibers. *Nat. Neurosci.* **2017**, *20*, 612–619. [CrossRef]
131. To, C.; Hellebrekers, T.; Park, Y.-L. Highly stretchable optical sensors for pressure, strain, and curvature measurement. In Proceedings of the 2015 IEEE/RSJ International Conference on Intelligent Robots and Systems (IROS), Hamburg, Germany, 17 December 2015; p. 5903.
132. Ahmad, O.S.; Bedwell, T.S.; Esen, C.; Garcia-Cruz, A.; Piletsky, S.A. Molecularly Imprinted Polymers in Electrochemical and Optical Sensors. *Trends Biotechnol.* **2019**, *37*, 294–309. [CrossRef]
133. Ertürk, G.; Mattiasson, B. Molecular Imprinting Techniques Used for the Preparation of Biosensors. *Sensors* **2017**, *17*, 288. [CrossRef]
134. Altintas, Z.; Pocock, J.; Thompson, K.-A.; Tothill, I.E. Comparative investigations for adenovirus recognition and quantification: Plastic or natural antibodies? *Biosens. Bioelectron.* **2015**, *74*, 996–1004. [CrossRef]
135. Pathak, A.K.; Limprapassorn, P.; Kongruttanachok, N.; Viphavakit, C. Molecularly Imprinted Polymer-Based Optical Sensor for Isopropanol Vapor. *J. Sens. Actuator Netw.* **2022**, *11*, 46. [CrossRef]
136. Lee, S.-W.; Ahmed, S.; Wang, T.; Park, Y.; Matsuzaki, S.; Tatsumi, S.; Matsumoto, S.; Korposh, S.; James, S. Label-Free Creatinine Optical Sensing Using Molecularly Imprinted Titanium Dioxide-Polycarboxylic Acid Hybrid Thin Films: A Preliminary Study for Urine Sample Analysis. *Chemosensors* **2021**, *9*, 185. [CrossRef]

137. Zhou, Y.; Xu, Y.; Xu, G.; Sugihara, O.; Cai, B. Molecularly Imprinted Polymer-Coated Optical Waveguide for Attogram Sensing. *ACS Appl. Mater. Interfaces* **2022**, *14*, 16727–16734. Available online: https://pubs.acs.org/doi/abs/10.1021/acsami.2c02362 (accessed on 6 August 2024). [CrossRef] [PubMed]
138. Xu, Y.; Zhou, Y.; Luo, H.; Li, H.; Ni, T.; Xu, G.; Sugihara, O.; Xie, J.; Cai, B. Molecularly imprinted polymer-coated hybrid optical waveguides for sub-aM fluorescence sensing. *Analyst* **2024**, *149*, 800–806. [CrossRef]
139. Antonini, M.-J.; Sahasrabudhe, A.; Tabet, A.; Schwalm, M.; Rosenfeld, D.; Garwood, I.; Park, J.; Loke, G.; Khudiyev, T.; Kanik, M.; et al. Customizing MRI-Compatible Multifunctional Neural Interfaces through Fiber Drawing. *Adv. Funct. Mater.* **2021**, *31*, 2104857. [CrossRef]
140. Lu, C.; Froriep, U.P.; Koppes, R.A.; Canales, A.; Caggiano, V.; Selvidge, J.; Bizzi, E.; Anikeeva, P. Polymer Fiber Probes Enable Optical Control of Spinal Cord and Muscle Function In Vivo. *Adv. Funct. Mater.* **2014**, *24*, 6594–6600. [CrossRef]
141. Yu, L.; Xuan, H.; Guo, Y.; Chin, A.L.; Tong, R.; Pickrell, G.; Wang, A.; Jia, X. Porous polymer optical fiber fabrication and potential biomedical application. *Opt. Mater. Express* **2017**, *7*, 1813–1819. [CrossRef]
142. Qu, Y.; Bartolomei, N.; Lagier, M.; Nguyen-Dang, T.; Page, A.G.; Yan, W.; Gupta, T.D.; Sorin, F. Stretchable Optical Fibers via Thermal Drawing. In Proceedings of the Advanced Photonics 2018 (BGPP, IPR, NP, NOMA, Sensors, Networks, SPPCom, SOF), Zurich, Switzerland, 2–5 July 2018; Optica Publishing Group: Washington, DC, USA, 2018; p. SoW1H.3.
143. Banerjee, H.; Bartolomei, N.; Song, J.; Sorin, F. Soft, stretchable optical fibers via thermal drawing. *EPJ Web Conf.* **2023**, *287*, 10003. Available online: https://www.epj-conferences.org/articles/epjconf/abs/2023/13/epjconf_eosam2023_10003/epjconf_eosam2023_10003.html (accessed on 6 August 2024). [CrossRef]
144. Beckers, M.; Schlüter, T.; Vad, T.; Gries, T.; Bunge, C.-A. An overview on fabrication methods for polymer optical fibers. *Polym. Int.* **2015**, *64*, 25–36. Available online: https://scijournals.onlinelibrary.wiley.com/doi/abs/10.1002/pi.4805 (accessed on 6 August 2024). [CrossRef]
145. Gallichi-Nottiani, D.; Pugliese, D.; Giovanna Boetti, N.; Milanese, D.; Janner, D. Toward the fabrication of extruded microstructured bioresorbable phosphate glass optical fibers. *Int. J. Appl. Glass Sci.* **2020**, *11*, 632–640. [CrossRef]
146. Talataisong, W.; Ismaeel, R.; Sandoghchi, S.R.; Rutirawut, T.; Topley, G.; Beresna, M.; Brambilla, G. Novel method for manufacturing optical fiber: Extrusion and drawing of microstructured polymer optical fibers from a 3D printer. *Opt. Express* **2018**, *26*, 32007–32013. [CrossRef]
147. Bonefacino, J.; Tam, H.-Y.; Glen, T.S.; Cheng, X.; Pun, C.-F.J.; Wang, J.; Lee, P.-H.; Tse, M.-L.V.; Boles, S.T. Ultra-fast polymer optical fibre Bragg grating inscription for medical devices. *Light. Sci. Appl.* **2018**, *7*, 17161. [CrossRef]
148. Dash, J.N.; Cheng, X.; Gunawardena, D.S.; Tam, H.-Y. Rectangular single-mode polymer optical fiber for femtosecond laser inscription of FBGs. *Photon. Res.* **2021**, *9*, 1931–1938. [CrossRef]
149. Van Hoe, B.; Van Steenberge, G.; Bosman, E.; Missinne, J.; Geernaert, T.; Berghmans, F.; Webb, D.; Van Daele, P. Optical fiber sensors embedded in flexible polymer foils. *Proc. SPIE* **2010**, *7726*, 772603. Available online: https://www.spiedigitallibrary.org/conference-proceedings-of-spie/7726/772603/Optical-fiber-sensors-embedded-in-flexible-polymer-foils/10.1117/12.854865.short (accessed on 1 May 2024).
150. Pisco, M.; Galeotti, F.; Quero, G.; Grisci, G.; Micco, A.; Mercaldo, L.V.; Veneri, P.D.; Cutolo, A.; Cusano, A. Nanosphere lithography for optical fiber tip nanoprobes. *Light. Sci. Appl.* **2017**, *6*, e16229. [CrossRef]
151. Hassan, H.U.; Bang, O.; Janting, J. Polymer Optical Fiber Tip Mass Production Etch Mechanism to Achieve CPC Shape for Improved Biosensor Performance. *Sensors* **2019**, *19*, 285. [CrossRef] [PubMed]
152. Manocchi, A.K.; Domachuk, P.; Omenetto, F.G.; Yi, H. Facile fabrication of gelatin-based biopolymeric optical waveguides. *Biotechnol. Bioeng.* **2009**, *103*, 725–732. [CrossRef] [PubMed]
153. Kee, J.S.; Poenar, D.P.; Neuzil, P.; Yobas, L. Design and fabrication of Poly(dimethylsiloxane) single-mode rib waveguide. *Opt. Express* **2009**, *17*, 11739–11746. [CrossRef]
154. Sharma, K.; Morlec, E.; Valet, S.; Camenzind, M.; Weisse, B.; Rossi, R.M.; Sorin, F.; Boesel, L.F. Polydimethylsiloxane based soft polymer optical fibers: From the processing-property relationship to pressure sensing applications. *Mater. Des.* **2023**, *232*, 112115. [CrossRef]
155. Bruck, R.; Hainberger, R. Polymer waveguide based biosensor. *Proc. SPIE* **2008**, *7138*, 71380N. [CrossRef]
156. Arkwright, J.W.; Blenman, N.G.; Underhill, I.D.; Maunder, S.A.; Szczesniak, M.M.; Dinning, P.G.; Cook, I.J. In-vivo demonstration of a high resolution optical fiber manometry catheter for diagnosis of gastrointestinal motility disorders. *Opt. Express* **2009**, *17*, 4500–4508. [CrossRef]
157. Wang, D.H.-C.; Abbott, A.; Maunder, S.A.; Blenman, N.G.; Arkwright, J.W. A miniature fiber Bragg grating pressure sensor for in-vivo sensing applications. In Proceedings of the OFS2012 22nd International Conference on Optical Fiber Sensors, SPIE, Edinburgh, UK, 15–19 October 2012; Volume 8421, pp. 656–659.
158. Arkwright, J.W.; Underhill, I.D.; Maunder, S.A.; Blenman, N.; Szczesniak, M.M.; Wiklendt, L.; Cook, I.J.; Lubowski, D.Z.; Dinning, P.G. Design of a high-sensor count fibre optic manometry catheter for in-vivo colonic diagnostics. *Opt. Express* **2009**, *17*, 22423–22431. [CrossRef]
159. Voigt, S.; Rothhardt, M.; Becker, M.; Lüpke, T.; Thieroff, C.; Teubner, A.; Mehner, J. Homogeneous catheter for esophagus high-resolution manometry using fiber Bragg gratings. In Proceedings of the Optical Fibers and Sensors for Medical Diagnostics and Treatment Applications X., February 2010, San Francisco, CA, USA, 23–28 January 2010; SPIE: Bellingham, WA, USA, 2010; Volume 7559, pp. 61–70.

160. Becker, M.; Rothhardt, M.; Schröder, K.; Voigt, S.; Mehner, J.; Teubner, A.; Lüpke, T.; Thieroff, C.; Krüger, M.; Chojetzki, C.; et al. Characterization of fiber Bragg grating-based sensor array for high resolution manometry. In Proceedings of the Optical Sensing and Detection II, SPIE Photonics Europe. Bellingham, WA, USA, 16–19 April 2012; 2012; Volume 8439, pp. 15–23.
161. Ulacia, P.; Rimac, G.; Lalancette, S.; Belleville, C.; Mongrain, R.; Plante, S.; Rusza, Z.; Matsuo, H.; Bertrand, O.F. A novel fiber-optic based 0.014″ pressure wire: Designs of the OptoWire^{TM}, development phases, and the O_2 first-in-man results. *Catheter. Cardiovasc. Interv.* **2020**, *99*, 59–67. [CrossRef] [PubMed]
162. Dennison, C.R.; Wild, P.M. Enhanced sensitivity of an in-fibre Bragg grating pressure sensor achieved through fibre diameter reductiosn. *Meas. Sci. Technol.* **2008**, *19*, 125301. [CrossRef]
163. Friedemann, M.; Voigt, S.; Mehner, J. Pressure sensor catheter based on Fiber Tip Fabry-Pérot-Interferometer and Fiber Bragg Grating for temperature compensation: Fiber-optic hybrid sensor catheter for invasive pressure measuring. *Curr. Dir. Biomed. Eng.* **2022**, *8*, 404–407. [CrossRef]